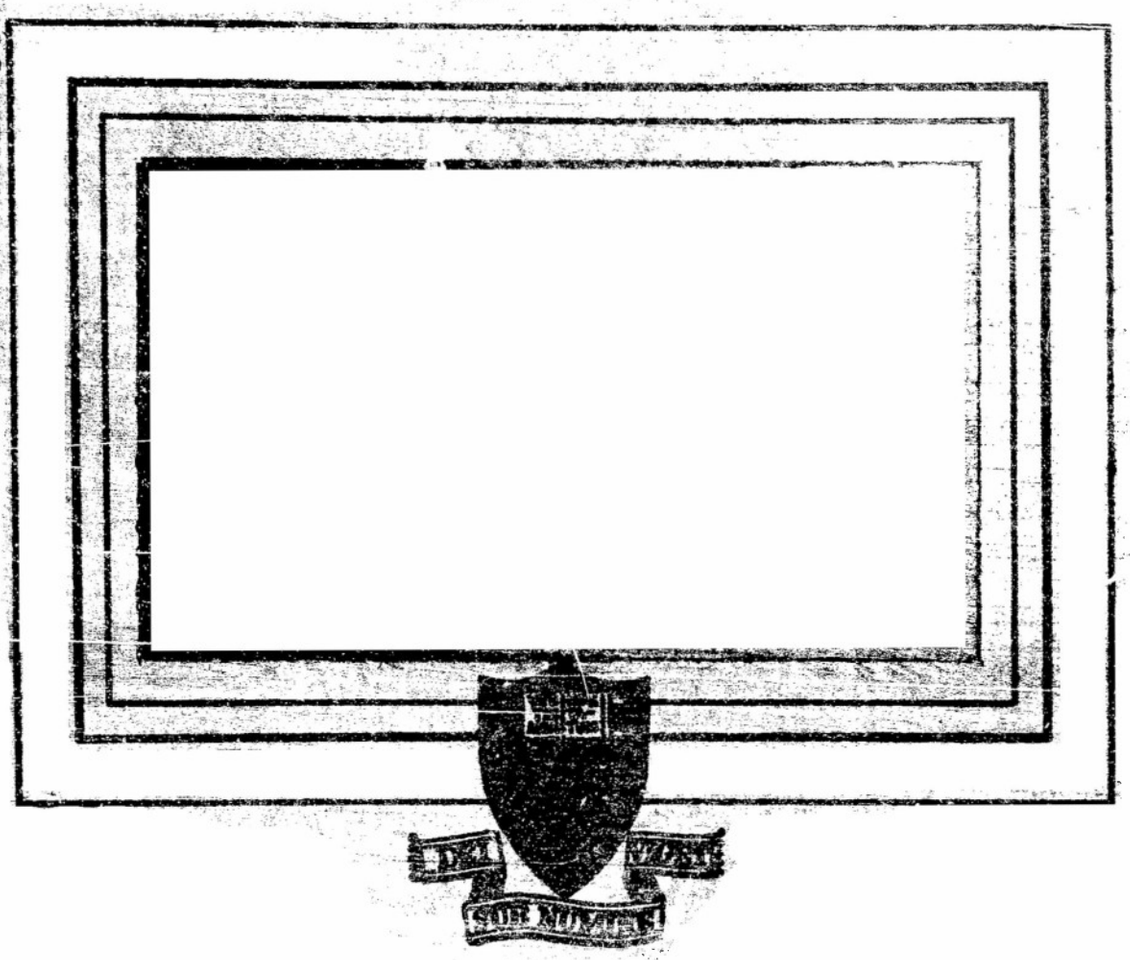

PRINCETON UNIVERSITY

DEPARTMENT OF AERONAUTICAL ENGINEERING

PRELIMINARY REPORT ON CIRCULATION CONTROL BY MEANS OF TRAILING EDGE SUCTION AND THE CUSP EFFECT

By

D. C. Hazen
R. F. Lehnert
T. E. Sweeney
F. O. Ringleb

REPORT No. 234 JUNE 15, 1953

OFFICE OF NAVAL RESEARCH

CONTRACT NO. N6-onr-27016

Project No.NR 212-011

As it is felt that the general results and conclusions reached after two years of research devoted to an investigation of circulation control by means of trailing edge suction and particularly the development of the cusp effect may be of interest to people working in allied fields, a preliminary report has been prepared. A full report including all experimental data is being compiled and will be issued in approximately two months.

LIST OF ILLUSTRATIONS

TABLE OF CONTENTS

REFERENCES

1. Regenscheit, B. On a New Application of Suction for the Increase of Lift of an Airfoil, FB 1474 (1941)

2. Smith, C. B. Summary of Analysis of Trailing Edge Suction Slot - United Aircraft Corporation Inter-Company Report (1948)

3. Ehlers, F. On the Influence of Sinks on the Lift and Pressure Distribution of Airfoils with Suction Slots. MAP -VG 67 189 T (1946)

4. Ringleb, F.O. Theory and Application of the Flow Over a Cusp, Princeton Report No. 192 (1952)

SUMMARY

A systematic investigation of circulation control systems; that is, systems employing powered or automatically controlled flow singularities to produce high lift without a corresponding change in angle of attack, especially those systems utilizing suction at the trailing edge, is reported. A mathematical method for the prediction of the performance of such systems under certain limited conditions is presented. The development of the use of the stable trapped vortex formed in a cusp-like shape for circulation control purposes is also reported and a few possible applications indicated.

INTRODUCTION

The necessity of producing high lift at low speeds is becoming increasingly evident in both military and commercial aircraft application. The problems of carrier landings and take-offs have now or very shortly will become so great that there is little hope of solving them completely by improved catapult and arresting gear design. The minimum flight speeds of aircraft have been steadily increasing as the design trends have been for ever larger, heavier and faster aircraft. If such aircraft are to be operated off our existing carriers, some method must be found to reduce their minimum flight speed.

If one examines the relationship between the lift produced by the wing and the minimum flight or stalling speed

$$V_S = \sqrt{\frac{2\,W/S}{\rho\, C_{L\,max}}} \qquad (1)$$

it immediately becomes apparent that for a given aircraft operating at a given gross weight, the only way in which this speed can be reduced is by an increase in maximum lift coefficient.

There are, in general, only two methods by which the maximum lift coefficient of a wing may be increased. The first of these consists of influencing the air flowing over the profile in some manner so as to delay or prevent separation; i.e., stall, thereby allowing the angle of attack to be increased hence increasing lift. The second method consists of inducing a change in the circulation about a profile without a change in angle of attack. From the Kutta-Joukowski relation

$$l = \rho V \Gamma \qquad (2)$$

it will be seen that an increase in circulation results in a corresponding increase in lift.

Conventional aircraft of today employ systems which utilize either or both of these methods. The slot or slat located at the leading edge energizes the boundary layer and delays separation, while the flap alters the camber of the profile, thus changing the circulation and resulting in a higher lift without a corresponding change in angle of attack. These effects are shown by Figure 1.

The main disadvantage of the slot as a high lift device is that it produces its lift at a high angle of attack, frequently creating severe visibility problems and penalizing the performance of the aircraft with a cumbersome and heavy landing

gear. The flap is in general a satisfactory device if one accepts high lift at the expense of added drag and heavy pitching moments.

It should be pointed out that an increase of drag is not an objectionable characteristic in the landing configuration as it permits a steeper angle of glide at a given speed than would otherwise be possible. It is however objectionable at take-off when high lift and low drag would be desirable. This indicates that control of the drag may well be as important as the control of lift.

As both the slot and the flap are limited to a relatively low amount of lift increase due to the flow separation, attempts have been made to increase the effectiveness of these systems by the addition of power. Boundary layer control systems work on much the same principal as the slot. By either energizing the boundary layer by blowing through slots or removing it when it thickens by sucking through slots, separation can be delayed until very high angles and values of lift can be obtained.

Figures 2, 3, and 4, are photographs taken in the Princeton University 14" x 2" smoke tunnel and show examples of this type of boundary layer control.

It must be pointed out that boundary layer control when properly applied can stabilize a laminar boundary layer, thus resulting in a decrease of aerodynamic drag, even when the power required to produce the control is considered. It must also be pointed out that the disadvantages of the slot still remain. Thus if such a system is to be used for high lift, a penalty is paid in visibility and landing gear weight.

Another approach to the problem has been the use of suction or blowing to cause the flow to adhere to a deflected flap. As such a system can produce values of lift frequently double that resulting from the deflection of the flap alone without any increase in angle of attack, it is properly referred to as circulation control. It is clear that such a system must have an effect on the boundary layer, but this is not its major function nor is this effect nearly as pronounced as on a system designed to utilize Boundary Layer Control because the slots are usually located in a turbulent boundary layer region and hence are relatively ineffective from a stabilization point of view.

When a circulation control system of this type is employed, the wing normally starts to stall due to a laminar separation starting at the leading edge. If one can afford the additional weight and complication, porous suction control of the boundary layer, particularly at the leading edge, allows extremely high angles of attack to be attained without stall. As the lifts produced by the two methods are additive, extremely high lifts can be obtained. Figures 5, 6, and 7 demonstrate this type of circulation control.

The first two years of the Princeton research program in this field of circulation control has been directed towards an investigation of a system first suggested by B. Regenscheit during the war. This system can be employed with a flap, but we have investigated it simply as the addition of a flow singularity to an existing profile. The system consists of nothing other than a suction slot

located at the trailing edge of the wing.

DISCUSSION

B. Regenscheit[1] was the first to observe that the effect on the increase of lift of suction through a slot located at the trailing edge of a wing profile is considerably larger than the effects obtained with the slot in any other location on the upper surface. This fact has been explained by C.B. Smith[2], who developed a relatively simple analysis by means of potential flow theory. Let the region outside of the profile be conformally transformed into the region outside of a circle with unit radius in such a way that the infinite points of both planes correspond. The portion of the profile surface between the trailing edge and the suction slot will thus correspond to an arc β on the circle. The lift increase Δc_l resulting from a given suction coefficient c_Q is obtained by this arc as shown by the relation

$$\Delta c_l = 2 \cot \frac{\beta}{2} \cdot c_Q \qquad (3)$$

This expression shows that for a given c_Q, Δc_l increases as β decreases; i.e., the lift increment increases as the slot location is moved towards the trailing edge.

Equation 3 is based on the assumption of two-dimensional irrotational frictionless flow of an incompressible medium and on the simplification that the suction is produced by a single sink situated within a small slot having parallel walls.

For low quantities of suction, the flow develops a stagnation point between the suction slot and the trailing edge (see Figure 8), thus resulting in a condition in which only flow from the upper surface enters the suction slot. As in the case of no suction, the Kutta-Joukowski hypothesis requires that another stagnation point be situated at the trailing edge. With increasing suction, the first of these stagnation points moves towards the trailing edge reaching this point for some certain value of c_Q.

Considerable interest has been created by the question of what flow picture results if c_Q is increased beyond this value. F. Ehlers[3] assumed that both stagnation points combined to move as a stagnation point of the second order to the lower side of the profile. However, from the standpoint of potential theory, an equally possible solution assumes that one of these stagnation points stays at the trailing edge while the other moves to the lower side, or yet another possibility is that both move to the lower side in separate positions. Finally, there is the possibility that both stagnation points combine and leave the trailing edge to form a stagnation point in the free stream.

Obviously, the determination of which of these possibilities can actually be expected in practice is of basic importance to the understanding of trailing edge suction. A smoke tunnel experiment at Princeton University showed the last case to be the solution with physical significance. Figure 9 shows

shows the observed free stream stagnation point. It will be seen that when this stagnation point occurs some flow proceeds around the lower lip of the trailing edge slot resulting in flow entering the slot from both the upper and lower surfaces of the profile. Unfortunately, it can be expected that this change in the character of the flow will result in a considerably diminished effect from trailing edge suction. Hence, unless measures are taken to prevent this motion of the stagnation points, the value of suction coefficient which causes the two stagnation points to combine at the trailing edge can be considered the practical upper limit for this means of increasing lift.

In accordance with the assumptions upon which the theory is based, equation 3 can be applied without further considerations to the case of trailing edge suction only if there is a small suction slot with parallel walls at the profile surface near the trailing edge. Only under these conditions will the conformal transformation of the original profile furnish the correct angle β . Such a slot however, is not quite adequate in the case of suction at the trailing edge. Usually the rear of the profile is cut off so that the slot is bounded by a somewhat longer lip on the lower surface of the profile than on the upper. (See Figure 11)

The basic problem in this case is to determine the correct angle β which is to be substituted in this equation. For small values of β , as in the case of suction near the trailing edge, $\cot \beta/2$ changes rapidly with β . This results in a considerable sensitivity of the lift increase obtained with the suction slot arrangement. A solution to the problem of the determination of β can be solved by a relatively simple procedure of conformal mapping resulting in a good accordance between the computed lift and the lift obtained from pressure distribution and balance measurements.

1. General Theory of Circulaton Control by Suction Through a Slot

The developments presented in this section are based on the consideration of normal wing profile with a small suction slot located on the upper surface. As previously mentioned, it will be assumed that this slot has parallel straight walls, and that suction is produced by a sink S situated within this slot. To satisfy continuity requirements, a source of equal strength must then be assumed to be located at infinity. It is further assumed that the profile is situated at an angle of attack α in a uniform flow field having the velocity w_∞ at infinity. Figure 10 indicates the resulting flow field for a moderate suction quantity. For this suction quantity a stagnation point P appears on the upper surface of the profile between the suction slot and the trailing edge. (This case is also illustrated by Figure 8.) The flow smoothly leaves the trailing edge, indicating the presence of a stagnation point attached to the profile at this point and hence the Kutta-Joukowski condition is satisfied as in the case of no suction. A third stagnation point is, of course, situated near the nose of the profile.

The two dimensional potential flow of an incompressible medium satisfying these conditions can be determined in the same manner as the flow about a profile without suction as in classical aerodynamics. To do this, the outside of the pro-

file in the $z = x + iy$ -plane is transformed conformally to the outside of a circle of unit radius in the $\zeta = \xi + i\eta$ -plane in such a way that the infinite points of the two planes correspond and that the size and position of the profile in the z-plane is such that $\frac{dz}{d\zeta} = 1$ for $\zeta \to \infty$ and $\zeta = 1$

corresponds to the trailing edge of the profile. (See Figure 10) Under these conditions, the transformation is determined uniquely and the region outside of the circle $|\zeta| = 1$ has an expansion of the form

$$z = f(\zeta) = \zeta + \frac{c_1}{\zeta} + \frac{c_2}{\zeta^2} + \cdots \tag{4}$$

Under the restrictions of the transformation, the x-axis corresponding to $\alpha = 0$ is at the same time the axis of zero lift without suction. The length of the profile is determined by the transformation and has a value approximately equal to 4.

As a result of the transformation, a well-defined point $\zeta = e^{i\beta}$ where β is the arc of the circle between the points corresponding to the trailing edge and the slot, corresponds to the slot exit on the profile. More rigorously, the point determined by β in fact corresponds to the sink within the slot, and the slot walls correspond to two small arcs adjacent to β if the inside of the slot is included in the transformation. If,however, the slot is considered infinitesimally small, β defines a point which corresponds to the slot including the sink as a limit.

The flow in question is determined by the complex potential function.

$$\chi = w_\infty \left(\zeta e^{-i\alpha} + \frac{1}{\zeta e^{-i\alpha}}\right) + \frac{\Gamma i}{2\pi} \ln \zeta + \frac{Q}{2\pi}\left(\ln \zeta - 2\ln(\zeta - e^{i\beta})\right) \tag{5}$$

The first term represents the parallel flow at an angle of attack α around the circle, the second term a circulation (vortex) around the circle with strength Γ. The third term results from a source with the strength Q at $\zeta = 0$, a source of equal strength at $\zeta = \infty$ and a sink with the strength $-2Q$ at $\zeta = e^{i\beta}$ so that the strength of this sink with respect to the flow outside the circle is equal to $-Q$, where Q is measured in units of volume per unit span and time. The source at $\zeta = 0$ inside the circle is added in order to obtain the contour of the circle as a streamline. The flow represented by $\chi = \chi(\zeta)$ is transformed by $z = f(\zeta)$ to a flow with corresponding singularities in the plan of the profile.

The complex velocity function may be expressed as

$$\frac{d\chi}{dz} = \frac{1}{f'(\zeta)} \frac{d\chi}{d\zeta} = w e^{-i\theta} \tag{6}$$

where $f'(\zeta) = dz/d\zeta$, w is the velocity and θ the direction of the flow at a point in the z-plane. Thus, for a stagnation point in the z-plane $\frac{d\chi}{dz} = 0$.

Hence for a point

$$\zeta = e^{i\gamma}$$

to correspond to a stagnation point on the profile $\frac{dz}{d\zeta}$ must equal zero at the point with the further condition that $f'(\zeta) = dz/d\zeta$ is not zero or is at least of smaller order zero than $dz/d\zeta$. Accordingly, if equation 5 is differentiated with respect to ζ and ζ replaced by $e^{i\gamma}$, one obtains after some trigonometric operations the relation

$$\Gamma = 4\pi w_\infty \sin(\alpha - \gamma) + Q \cot \frac{\beta - \gamma}{2} \tag{7}$$

Where the angle γ determines the position of any stagnation point. Since the point $\zeta = 1$ ($\gamma = 0$) is supposed to be a stagnation point in accordance with the Kutta-Joukowski condition, the relationship simplifies to

$$\Gamma = 4\pi w_\infty \sin\alpha + Q \cot \beta/2 \tag{8}$$

Thus the circulation is determined by the velocity w_∞, the angle of attack α, the position β and the strength Q of the sink.

The suction coefficient C_Q is generally defined as

$$C_Q = \frac{Q}{S w_\infty} \tag{9}$$

where S is the wing area, w_∞ the free stream velocity and Q the volume of suction per unit time. In our preceding discussion a unit span has been supposed, thus if c is the profile chord length c_Q may be defined as

$$c_Q = \frac{Q}{c w_\infty}$$

where c is approximately equal to four. If Γ is now eliminated from equations 7 and 8, one obtains the coefficient

$$c_Q = \frac{-4\pi \sin(\alpha - \gamma) - \sin\alpha}{c \cot\frac{\beta - \gamma}{2} - \cot\frac{\beta}{2}}$$

which simplifies to

$$c_Q = \frac{8\pi}{c} \cos\left(\alpha - \frac{\gamma}{2}\right) \sin\frac{\beta}{2} \sin\frac{\beta - \gamma}{2} \tag{10}$$

From this relation one can determine how the stagnation point between the suction slot and the trailing edge point defined by γ moves with changing c_Q.

As previously explained, a case of special interest occurs when c_Q is increased sufficiently to cause this stagnation point to reach the trailing edge. In this case γ reaches the limit zero and one obtains the value

$$c_Q^* = \frac{8\pi}{c} \cos\alpha \sin^2 \beta/2 \tag{11}$$

This special suction coefficient can be considered as the highest suction coefficient for which tralling edge suction is economical.

The components X and Y of the force which acts on the outside of the profile due to the pressures produced by the flow can be determined from Blasius' equation.

$$Y + iX = -\frac{\rho}{2} \oint_C \left(\frac{dx}{dz}\right)^2 dz \qquad (12)$$

where ρ is the density of the fluid. In this particular case, the curve of integration C which must be considered, is the surface contour of the profile up to the slot, the parallel sides of the slot up to a perpendicular connection between them and this connection itself. When transformed into the ζ-plane, equation 12 becomes

$$Y + iX = -\frac{\rho}{2} \oint_K \left(\frac{dx}{d\zeta}\right)^2 \Big/ \frac{dz}{d\zeta} \, d\zeta \qquad (13)$$

The curve of integration K now consists of the circle $|\zeta| = 1$ up to a small half circle excluding the point $\zeta = e^{i\beta}$ from the outside region and of this small half circle itself, which corresponds to the connection of the slot walls. This curve K can be deformed into a large circle around $\zeta = 0$ because there are no singularities of the integrand outside K except those at infinity.

If equation 5 is differentiated and substituted into equation 13, the resulting integral can be evaluated by expanding the integrand into a power series of $\frac{1}{\zeta}$ where only the term with the first power of $\frac{1}{\zeta}$ gives a value which is not equal to zero. This computation which is omitted here results in the following expression.

$$Y + iX = \rho w_0 (\Gamma + Qi) e^{-i\alpha} \qquad (14)$$

The components of this force parallel and perpendicular to the free stream direction are the drag d and the lift l respectively. Therefore

$$l + id = (Y + iX) e^{i\alpha}$$
$$= \rho w_0 (\Gamma + Qi)$$

Thus

$$l = \rho w_0 \Gamma \quad , \quad d = \rho w_0 Q \qquad (15)$$

This result has been derived by C. B. Smith [2].

If the value of Γ from equation 8 is substituted into equation 15 for the lift obtains

$$l = \rho w_0 (4\pi w_0 \sin\alpha + Q \cot\tfrac{\beta}{2}) \qquad (16)$$

Using the definition of the lift coefficient

$$c_{\zeta} = \frac{1}{\rho/2\, w_0^2\, c} \tag{17}$$

and c_Q from equation 9a, equation 16 becomes

$$c_{\zeta} = \frac{8\pi}{c} \sin\alpha + 2 c_Q \cot \frac{\beta}{2} \tag{18}$$

This result shows that the lift coefficient consists of the lift coefficient $8\pi/4 \sin\alpha$ as predicted for the zero suction case by classical aerodynamics plus a term

$$\Delta c_{\zeta} = 2 c_Q \cot \frac{\beta}{2} \tag{19}$$

due to suction.

When the stagnation point P reaches the trailing edge, the expression for the lift increase becomes

$$\Delta c_{\zeta}^{*} = 2\pi \cos\alpha \sin\beta \tag{20}$$

which represents the upper practical limit for trailing edge suction.

2. Determination of β in the Case of Trailing Edge Suction.

If the suction slot is small and enters the surface of a given profile with parallel walls, the value of β can be found by the conformal mapping of the profile into a circle as described previously. If, however, as is usually the case of trailing edge suction, the tail of the profile has been cut off so that the edges of the upper and lower surfaces form the slot entrance, then the conformal mapping of the original profile will not lead to a correct determination of β. In this case, the profile with the slot has to be considered as a new profile like that of Figure 11, the situation of the real slot being indicated by an arrow.

In this situation, the following procedure is to be recommended. The edge of the longer lip of the trailing edge (usually the lower lip) is connected by a straight line to the mid-point of the radius connecting the center of curvature of the nose with the nose point. This straight line is then considered as a slot and the region surrounding it is transformed conformally to the region outside a circle. If the straight line connects the points $z = -R$ and $z = +R$ in the plane of the profile, the transformation to be applied is the inverse transformation of

$$z = \frac{1}{2}\left(\zeta + \frac{R^2}{\zeta}\right)$$

(the Joukowski transformation) or

$$\zeta = z + \sqrt{z^2 - R^2} \tag{21}$$

This transformation is frequently applied in order to transform a profile into a nearly circular curve. The numerical computation of $\zeta = \xi + i\eta$ as a function of $z = x + iy$ can be performed by computing $\cosh\theta$ from the relation

$$\cosh^2\theta = \frac{1}{2}\left(\frac{x^2+y^2}{R^2} + 1\right) + \sqrt{\frac{1}{4}\left(\frac{x^2+y^2}{R^2} + 1\right)^2 - \frac{x^2}{R^2}} \tag{22}$$

Knowing $\cosh \Theta$ we may apply the relations

$$\cos\phi = \frac{X}{R\cosh\Theta} \tag{23}$$

and

$$\gamma = Re^{\Theta} \tag{24}$$

then

$$\xi = \gamma\cos\phi \qquad \eta = \gamma\sin\phi \tag{25}$$

Figure 12 shows the transformed profile-points for the case of Figure 11 where the tail of a NACA 23015 profile has been cut away from 10% chord length on the upper side to 5% on the lower.

The transformed profile is now approximated by two tangential circular arcs, one ending at the upper edge A and the other ending at the point $\xi = R$. Both arcs are tangent at a point C somewhere near the point corresponding to the profile nose. A third circle orthogonal to these two passing through A and C is now considered. This circle (in this example a straight line) intersects the upper arc RC at the point B. The arc AB now corresponds to a curve in the z-plane which closes the profile by connecting the edge of the upper lip with a point on the line between $-R$ and R forming the upper boundary of the lower lip. This connection is perpendicular to both lips and can as an approximation be replaced by a small circular arc. On this connection the slot entrance S (sink) with parallel sides is assumed as indicated by the arrow in Figure 12. This configuration corresponds very closely to the normal geometry in the case of trailing edge suction.

A transformation by reciprocal radius with C as the center is now used to map the outside of the area bounded by the three arcs into a half plane with a rectangular step. (See Figure 13). This stepped half plane can be conformally transformed by use of the Schwarz-Christoffel transformation into a half plane. If $t = t_1 + i t_2$ is the complex coordinate in the halfplane and $s = s_1 + i s_2$ the complex coordinate in the stepped halfplane as indicated by Figure 13, the transformation is

$$s = \int_0^t \sqrt{\frac{t+1}{t}}\, dt$$

$t = 0$ and $t = -1$ are the points corresponding to the corners of the step. Integration of this expression yields

$$s = \sqrt{t+t^2} + \ln\left(\sqrt{t} + \sqrt{1+t}\right) \tag{26}$$

From this, one sees that $s = 0$ corresponds to $t = 0$ and $s = \frac{\pi}{2}i$ to $t = -1$.

In order to compute this transformation, it is convenient to introduce a new complex variable τ defined by the relation

$$\sqrt{t} + \sqrt{1+t} = \tau \tag{27}$$

Hence:

$$\sqrt{\zeta} = \frac{1}{2}\left(\gamma - \frac{1}{\gamma}\right), \quad \sqrt{1+\zeta} = \frac{1}{2}\left(\gamma + \frac{1}{\gamma}\right)$$

and

$$\zeta = \frac{1}{4}\left(\gamma - \frac{1}{\gamma}\right)^2$$
$$s = \frac{1}{4}\left(\gamma^2 - \frac{1}{\gamma^2}\right) + \ln \gamma \qquad (28)$$

If we now let

$$\gamma = r e^{i\epsilon} \qquad (29)$$

one obtains the expressions

$$s_1 = \frac{1}{4}\left(r^2 - \frac{1}{r^2}\right)\cos 2\epsilon + \ln r \qquad (30a)$$

$$s_2 = \frac{1}{4}\left(r^2 + \frac{1}{r^2}\right)\sin 2\epsilon + \epsilon \qquad (30b)$$

and

$$t_1 = \frac{1}{4}\left(r^2 + \frac{1}{r^2}\right)\cos 2\epsilon - \frac{1}{2} \qquad (31a)$$

$$t_2 = \frac{1}{4}\left(r^2 - \frac{1}{r^2}\right)\sin 2\epsilon \qquad (31b)$$

The values of s corresponding to real values of $\zeta \geq 0$ can be found directly from equation 26 and are plotted in Figure 14. In order to obtain the values of γ which correspond to points on the straight line $s_1 = 0$ equation 30a must be used to compute ϵ as a function of the parameter r. The other three expressions, equations 30b and 31 a and b yield the values s_2, t_1 and t_2 as functions of the same parameter r. Figure 15 presents values of t_1 and t_2 plotted as functions of s_2. Figures 14 and 15 present sufficient information for the determination of β.

The ζ half-plane is now transformed into the region outside of a circle in such a way that infinity of the z-plane corresponds to the infinite point of the new plane. This can be done by a transformation by reciprocal radius with C′ as a center, where C′ is the point corresponding to C after the step transformation (Figure 12). In this manner, the real ζ- axis is transformed into a circle K.

The two inversions and the step transformation have to be constructed or computed for only the original points R and S (corresponding to the sink). Now if R′ and S′ are the images on the circle K with the center M then

$$\beta = \angle R'M S'$$

For the example of Figure 11 where the tail of the NACA 23015 profile has been cut off from 90% chord on the upper surface to 95% on the lower, the above method yields

$$\Delta c_l = 2 c_Q \cot \varrho/2 = 12.3 c_Q$$

In Figure 17, this theoretical result is compared with experimental pressure distribution measurements for $\alpha = 0°$. The actual trailing edge (1b) used in these measurements is shown in Figure 16. If trailing edge 1a of this figure where the lower lip reaches to the trailing edge and the upper lip is maintained at 90% chord, is used the theory yields

$$\Delta c_l' = 8.05 c_Q$$

A balance measurement for $\alpha = 0°$ is compared for this case with the theoretical result in Figure 18. In both cases the maximum Δc_l values attained are considerably lower than the corresponding Δc_l^* values, from which it may be concluded that the stagnation point P did not reach the trailing edge in these tests.

3. Computation of the Pressure Distribution

The methods described in the previous section may also be used to compute the pressure distribution. In this case, all the points of the profile transformed by the inverse Joukowski transformation, shown in Figure 12, must be further transformed by the reciprocal radius and step transformations. These transformations yield a set of points in the neighborhood of the circle K. By any of the well known transformations these points may be transformed into points on the circle K itself.

A simpler and not less accurate method is to use the conformal transformation of the original profile itself and to locate a suction slot at the point corresponding to $\zeta = e^{i\varrho}$ found by the preceding method. It is advisable to use this method particularly if the conformal transformation of the original profile is known as in the case of many of the NACA profiles.

In order to find the velocity of the flow, the expression

$$w = \left| \frac{d\chi}{dz} \right|$$

has to be computed by making use of equation 5 and the relationship $z = F(\zeta)$. Doing this, and utilizing the definition of c_Q the following expression results.

$$\frac{w}{w_0} = \frac{1}{|F'(\zeta)|} \left| 2\left[\sin(\phi - \alpha) + \sin\alpha\right] + \frac{2}{\pi} c_Q \left[\cot\frac{\phi - \varrho}{2} + \cot\frac{\varrho}{2}\right] \right| \qquad (32)$$

In this equation ϕ is the amplitude of the point $\zeta = e^{i\phi}$ corresponding to the profile point under consideration. It should be noted that the equation has been developed on the assumption that the chord c is equal to 4. Using this assumption, it is possible to express the ordinate as

$$X = 2\cos\phi$$

with only a small error. If the velocity distribution ω/ω_0 of the profile is known for the case without suction ($c_Q = 0$) for a given angle of attack α, the value of $|F'(\zeta)|$ can be found for any point $x = 2\cos\phi$ on the profile by use of equation 32. Equation 32 can then be used to obtain the velocity distribution ω/ω_0 for any c_Q, ρ and α. The pressure distribution is then obtained from the equation

$$\frac{\Delta p}{q} = 1 - \left(\frac{\omega}{\omega_0}\right)^2 \qquad (33)$$

In this manner the computed pressure distributions of Figure 19 and 20 have been obtained for comparison with the experimental measurements.

4. Experimental Investigation of Trailing Edge Suction.

The majority of the experimental work of this program was conducted in a 3½' x 5' subsonic wind tunnel equipped with an auxiliary throat reducing the 5' dimension to 18" to enable easy two-dimensional testing. Suction was obtained from an auxiliary stage compressor taken from an Allison V-1710 engine. This compressor, driven by a D.C. motor, was located outside the tunnel, and air was ducted from the model by the system of piping shown in Figure 21. In order to avoid effecting the balance readings by introducing loads from the blower ducting, a special coupling consisting of two ball and socket joints connected by piping containing a slip joint was employed. Flexible piping was used to connect this coupling to the ducts.

A typical model is shown in Figure 22. The interior of the model formed a large plenum chamber from which the air is exhausted through nozzles which lead to the blower duct connections. The trailing edge of the model is cut away so that the last 20% of the profile contour can be conveniently altered by the addition of trailing edge plates. The model that was used to collect the vast majority of the data was constructed of brass castings and had a chord of only 8". Other models, constructed to study pressure distributions and Reynolds Number effects were made of wood and had chords of approximately 16". (The base profile used in all tests was the NACA 23015, but different trailing edges frequently resulted in different after-profile contours and airfoil chords. All data were reduced using the actual measured chord length rather than the base chord.)

Figure 23 shows the trailing edge configurations that were tested. An examination of each, together with an explanation of the reasons behind the design chosen is of considerable value.

Trailing Edges 1a, 1b and 1c: These were the first shapes tested. These trailing edges represented the range of lower lip overhang over which it was felt that a detailed investigation was warranted. The upper surface was simply formed with a radius, for, although it was felt the slot shape would strongly influence the results, the design of what was considered the correct slot shape was not completed. In order to obtain as complete information as possible, balance readings, pressure distributions, wake surveys and slot velocity pressure distribution studies were made on these models. The slot velocity distribution investigation showed only very slight varia-

tions along the span and consequently this study was not made on the subsequent models.

The test results for these first three models indicated that the geometry of the trailing edges strongly influenced the maximum lift of the section. The highest lift was achieved with trailing edge 1-b which had more overhang than 1-c but less than 1-a as seen from Figure 23. Since the slot thickness varied for each of these cases it was thought that there might be an optimum ratio of overhang to slot thickness. Theory indicates that Δc_l increases as the slot approaches the T.E. of the base profile, consequently, it was thought that in the case of 1-c the ratio was far below the optimum. As a result this ratio was increased for trailing edge 2-b.

Trailing Edges 2b, 2d, 2e: Trailing edge 2 is the computed correct slot shape. This was first tested with lower lip b and the results were encouraging inasmuch as the Δc_l at low angles and low suction quantities was the best that had so far been achieved. The maximum lifts, however, were very disappointing. It was thought that flow around the lower lip might account for this, consequently trailing edges d and e were designed with a longer overhang to overcome this difficulty.

It is interesting to note that again the maximum lifts achieved with the section were with the moderate overhang (trailing edge 2-e) See Figure 24. It was thought that this might be the result of a flow separation at the slot inlet so trailing edge 2 was modified internally in an attempt to effect a cure. The results are discussed below.

Trailing Edges 4f and 5e: It will be noted in Figure 23 that trailing edge 4 has an internal cusp to aid in diffusing the flow inside the model and to prevent any disturbance from working upstream around the inlet contour. The bent up lower lip was an attempt to limit the stagnation point travel and provide easy entrance for air into the slot. The results were mediocre compared to 1-b, although it did show a higher maximum lift than 2-e.

Trailing edge 5-e is another application of the cusp to provide a more efficient inlet contour to the suction slot. The results were not outstanding either in maximum lift or in power required to remove the air; however, more recently acquired knowledge indicates that the cusp in trailing edge 5 was improperly designed. Its chief claim to fame is that trailing edge 5-e was probably the inspiration for the suction vortex airfoil section described in the next section.

Trailing Edges d-a and 1-g: These two sections were tested to determine the effect of extreme shapes such as the sharp upper lip on d-a. The maximum lift for this section is poor, but it does compare more favorably with some of the other models at a lower c_Q. See Figure 24.

The experience of testing these models revealed that there can be a substantial flow around the lower lip into the slot under certain conditions of α and c_Q, thus forming a free stream stagnation point. Trailing edge 1-g

was designed to resist this tendency, but the results indicate that 1-g is not as good as 1-b from which it was formed.

The testing program also included the measurement of pressure distributions about special models built to the geometry of 1-a and 1-b with which lifts by pressure distribution were correlated with lifts from the balance.

Drag Associated with Trailing Edge Suction:

Because of the difficulty of obtaining accurate values for drag tares, it was decided early in the program not to use balance drag indications. Accordingly, all drags were determined by pressure surveying the wake. Normally this yields the sectional drag coefficient, but when suction is applied to the section, there is an additional drag not reflected in the wake. This is the change in momentum across the section due to the removed air. When this is applied to the wake drag there is a considerable increase in total drag due to suction, even though the wake drag may go almost to zero as the turbulent wake is effectively swallowed by the suction slot. The procedure followed has been to compute the additional drag due to suction and add this correction to the wake drag. Thus the total drags all appear high; however, in a practical application the designer will have a great deal of latitude in his selection of a drag coefficient depending upon the direction and velocity he chooses to discharge the removed air to the free stream, thus presenting the possibility of a powerful drag control.

Pitching Moment Associated with Trailing Edge Suction:

The effect of trailing edge suction on pitching moment is pronounced and seems to be basically a function of shape, overhang and suction quantity. The No. 1 series of trailing edges is characterized by the pitching moment going negative with both increasing angle and increasing suction. As the overhang decreases, there appears a strong tendency for a discontinuity in the pitching moment curve at the higher angles of attack.

The pitching moments of the No. 2 and No. 5 series of trailing edges differ somewhat from those of the No. 1 series in that pitching moment goes negative as suction is applied and positive as angle of attack is increased. The net result is that for the range of C_Q tested, the pitching moments are negative, but the slope of the curve is positive.

Trailing edges 4-f and d-a have pitching moment curves that combine the characteristics of the above two groups, but variations in the slopes of the curves are somewhat more gentle than are those of the series 1 and 2 trailing edges.

In summation, it appears that the pitching moment characteristics of trailing edge suction are severe and that a real design problem exists in the application of these devices.

Power Required for Suction: In order to compare the various configurations tested, it is obvious that lift, drag, and pitch are but part of the information needed. In order to gain as clear an idea as possible of the relative merits

of the devices tested, it was decided to measure the total pressure drop across the trailing edge. This was easily done by the installation of two Kiel tubes inside the model and measuring the difference in their average pressure and the free stream total pressure. Thus a designer would be able to estimate very closely the power to move the air through the slot. This, of course, would be added to the power requirement for the ducting, valves and similar apparatus in a given installation.

5. Development of the Cusp Effect

One of the most interesting and potentially one of the most important developments of this program was the determination of a means whereby a vortex could be created and stabilized at a desired location. This discovery was first made as a result of a severe diffuser stall in the auxiliary two-dimensional throat of the wind tunnel. The turbulence created by the flow separation from the diffuser walls was so severe that it was unsafe to operate the tunnel.

Many attempts were made to remedy this effect with varying degrees of success. The addition of a splitter helped the condition greatly, but the turbulence was still far too great for successful testing. More splitters, as well as various combinations of splitters and screens were tried, but all resulted in increased power losses and very little change in the turbulence. These different configurations are illustrated by Figure 25.

The final solution to the problem involved building a new diffuser with a very much reduced expansion angle. At the end of this diffuser there is a very considerable jump in cross-sectional area. Attempts to simply dump the flow into this larger area were unsuccessful and the shape shown in Figure 26 was finally tested. The first test made with this configuration was immediately successful. The turbulence dropped to an acceptable level and the extreme power losses vanished.

Pressure distribution studies were made and indicated the existence of a trapped vortex within the cusp. These measurements are indicated by Figures 27 and 28. Tuft investigations show that this vortex existed only at the floor while another vortex at right angles to the floor vortex occupied the majority of the cusp. The most striking characteristic of this complex flow was that it was relatively smooth and free from turbulence.

As a result of these findings, the theoretical investigation presented in Reference 4 was started as well as an investigation of diffuser characteristics in a small two-dimensional tunnel. The results of the experimental study were discouraging, for although the splitters and screens behaved as predicted, in no case was it possible to obtain a pronounced cusp effect.

The next step in the experimental program was to find a way of creating and stabilizing the vortex. Due to our previous work with trailing edge suction, our first application took the form of a trailing edge control. The resulting shape was not seriously considered as a useful profile, but was simply a streamline body to which a cusp could be fastened. Figure 29 shows

the first body tested. The base profile in this case was a 15% laminar flow symmetrical profile. The cusp was installed with its upper lip at the 70% chord point of the base profile and a suction slot was installed at the lower lip. The results obtained with this body were of considerable interest. On the first model, only pressure distribution studies were made, but these were sufficient to show the characteristic of the flow. Figure 30 demonstrates the type of pressure distributions that were obtained. Figure 30A shows the profile at zero angle of attack (based on the symmetrical base profile). At this angle the lift was slightly negative as shown by the higher pressures occuring on the upper surface. Note the disturbance created by the cusp. As suction is increased, a considerable portion of the flow proceeds from the lower surface, giving rise to the pressure distribution shown in Figure 30B. Note that a mild vortex action is taking place within the cusp and that the circulation over the profile effected although only very weakly. As suction is further increased, the flow about the trailing edge increases until suddenly a value of C_Q is reached which causes a vigorous vortex to be established resulting in the increased circulation indicated in Figure 30C.

Since these original tests, further investigations have been made indicating considerably more efficient applications of the principal of the trapped vortex are possible. The most notable feature of the flow resulting from these vortex applications is the powerful manner in which the vortex affects the downwash pattern. In one application utilizing a differant cusp form and location it was possible to cause the flow to adhere to a profile at angle of attack of 120°, an extreme but illuminating example.

Work is continuing at Princeton University and has recently been started at other institutions on the problem of examining the basic mechanisms of the flow and increasing the concepts of application of the cusp or trapped vortex. It is felt that this cusp effect or "trapped vortex" represents a major advance in the problem of circulation control and is a means by which very high lift coefficients may be obtained.

CONCLUSIONS

As a result of the wind tunnel test program reported in this preliminary report, the following conclusions can be reached.

1. The lift that may be produced by a profile equipped with a trailing edge suction slot increases with increasing suction quantities up to a limiting value without an increase in angle of attack.

2. The limiting value that may be obtained is determined by the quantity of suction required to move the stagnation point appearing on the upper surface to the trailing edge.

3. When this suction quantity is applied, the stagnation point appears in the free stream and flow proceeds from both the upper and lower surfaces.

4. The lift that can be obtained with an unflapped profile utilizing trailing edge suction is strongly affected by slot width and trailing edge overhang, but not particularly by upper surface slot shape.

5. The lift can with fair accuracy be predicted by theoretical considerations.

6. In one rather special case, it was possible to extract energy from the air to drive a vortex within a cusp to obtain a free stream expansion through a wide angle without separation.

7. It is possible to entrap a vortex within a cusp shape by means of suction.

8. This vortex can be used to impart a strong downward momentum to the air and hence to produce a large circulation about a profile.

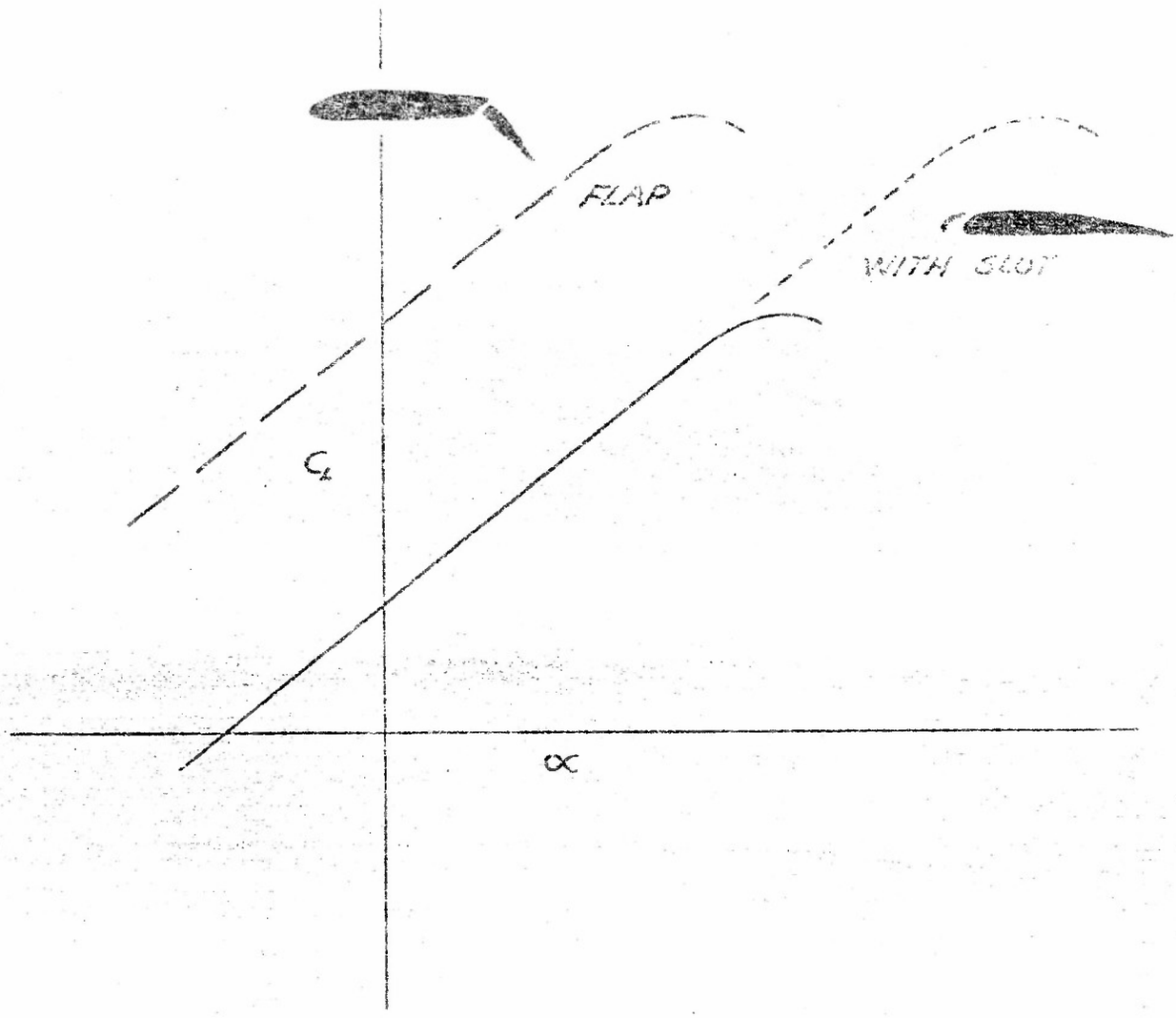

COMPARISON OF FLAP AND SLOT

Fig. 1

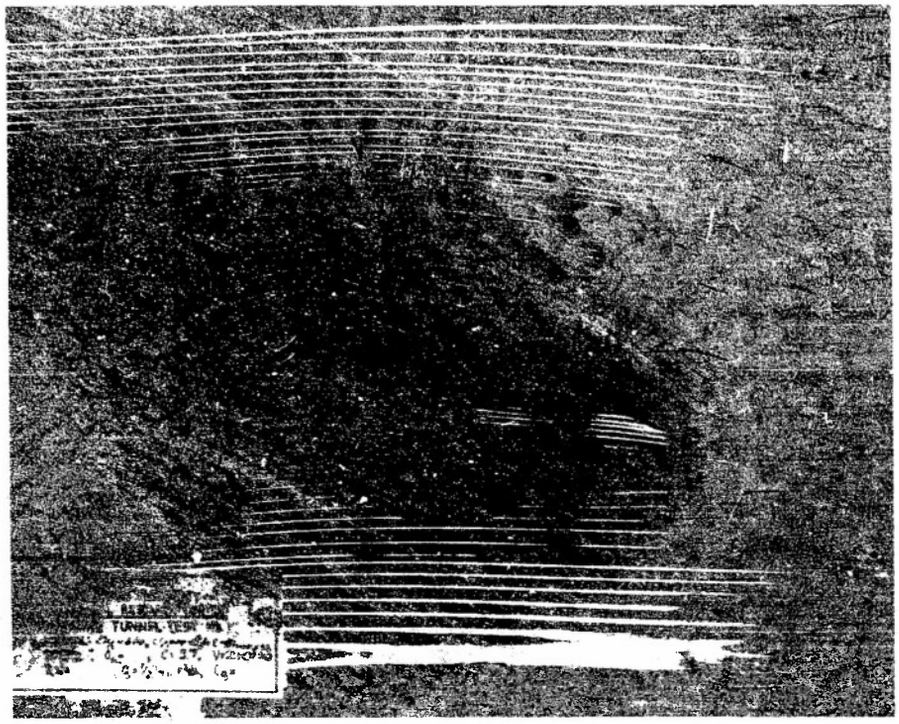

FIG. 2

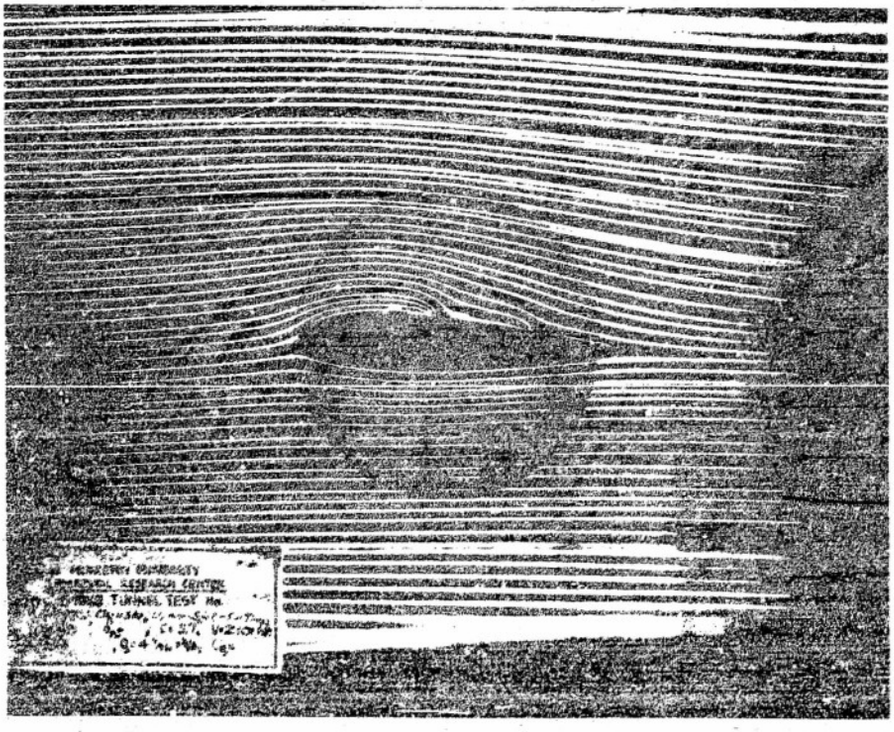

FIG. 3

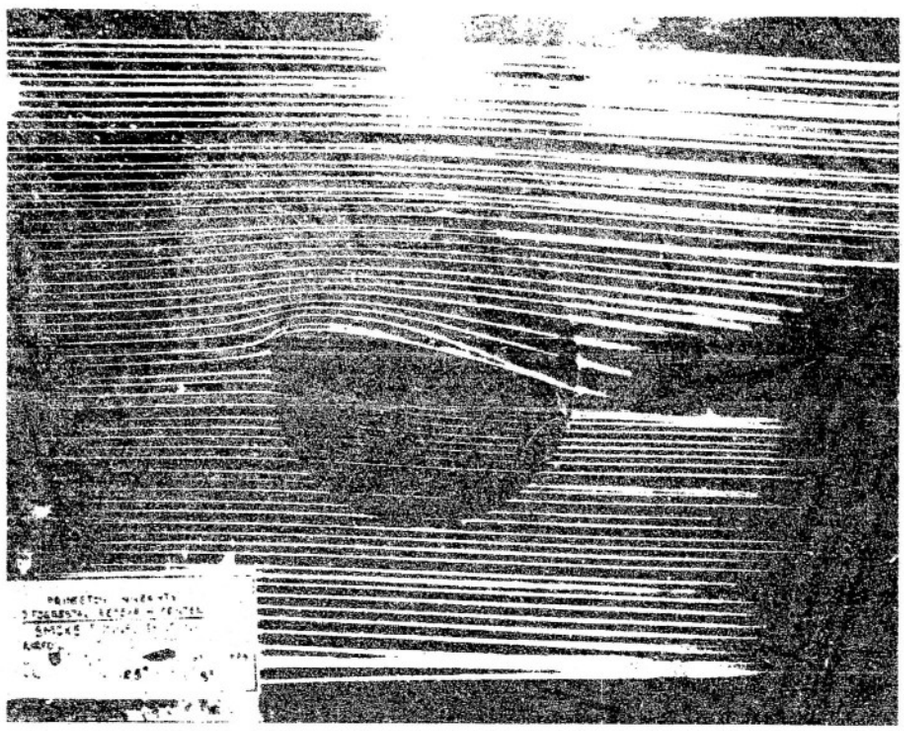

FIG. 4

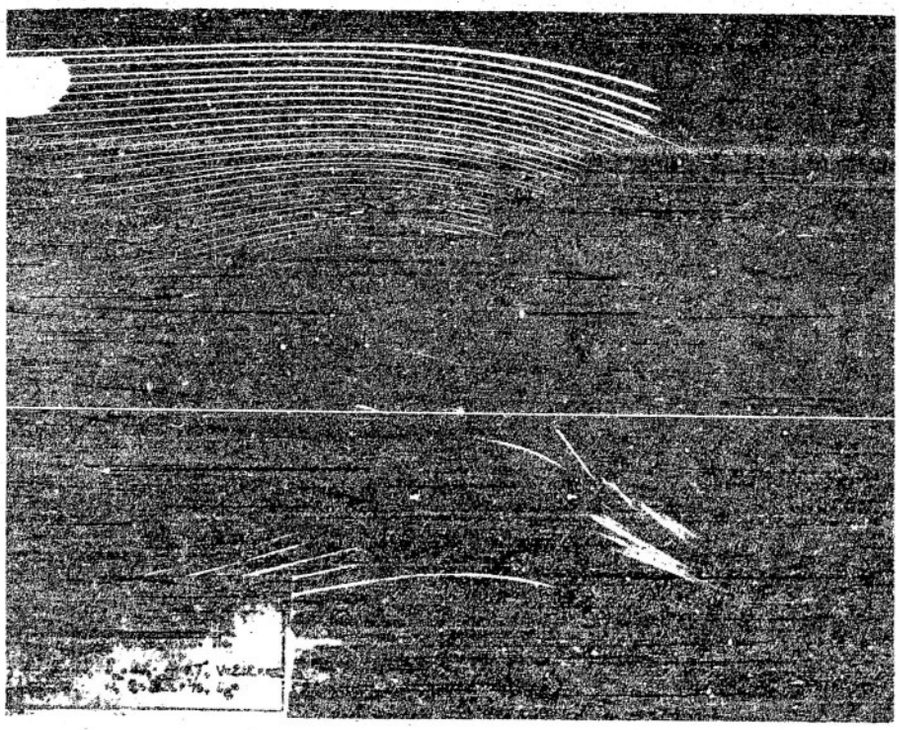

FIG. 5

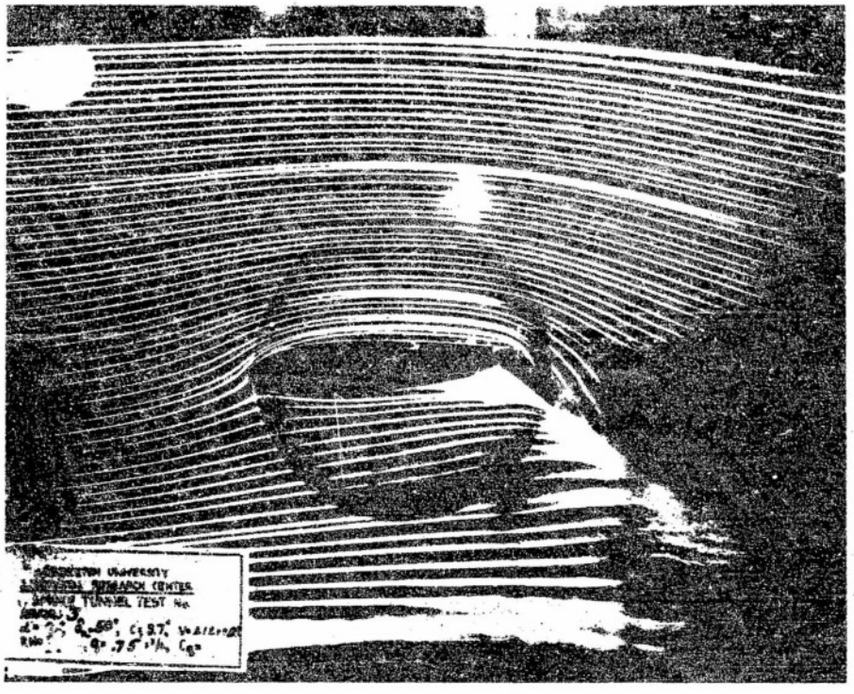

FIG. 6

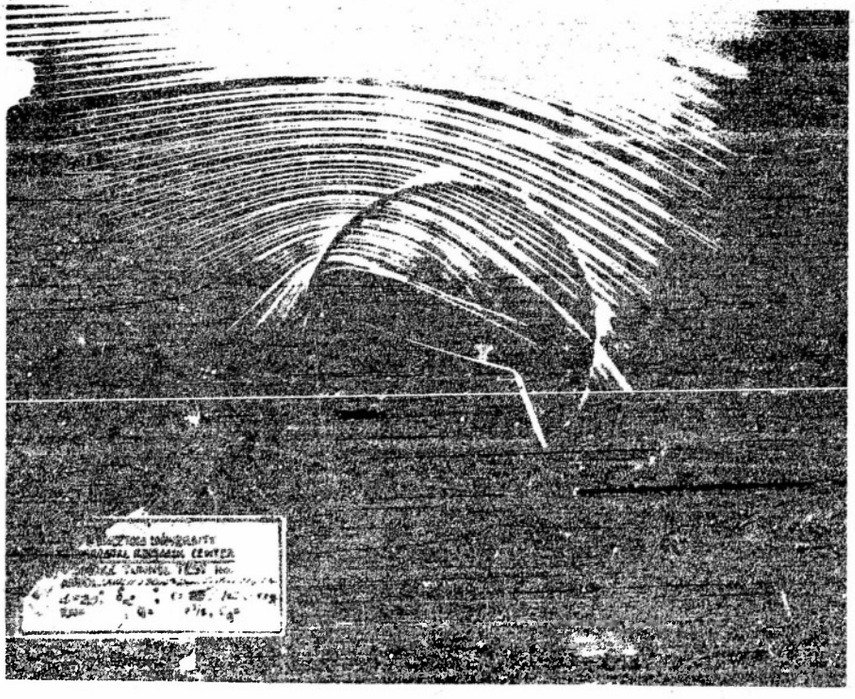

FIG. 7

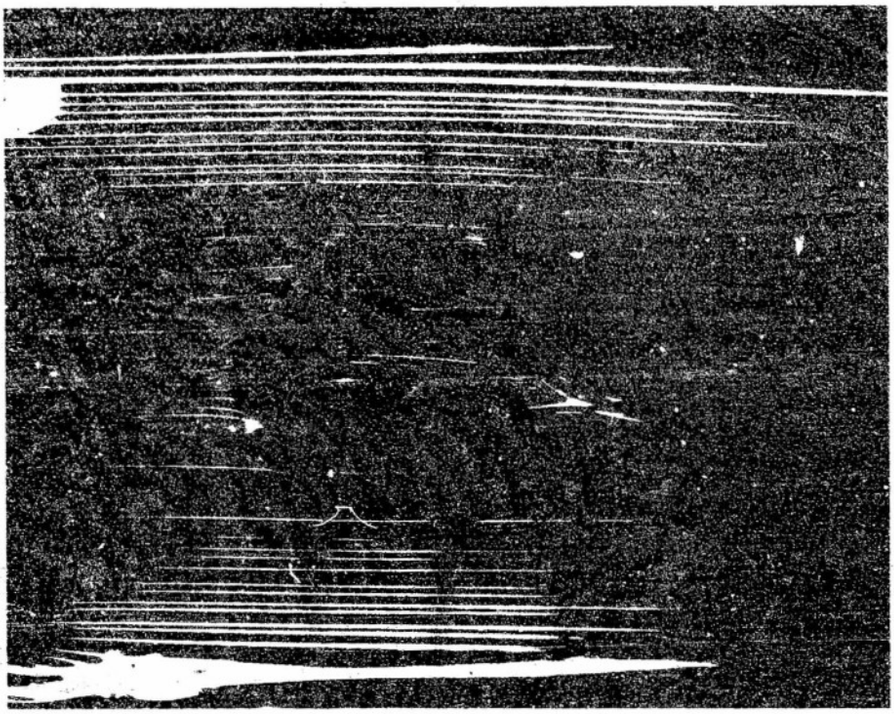

FIG. 8

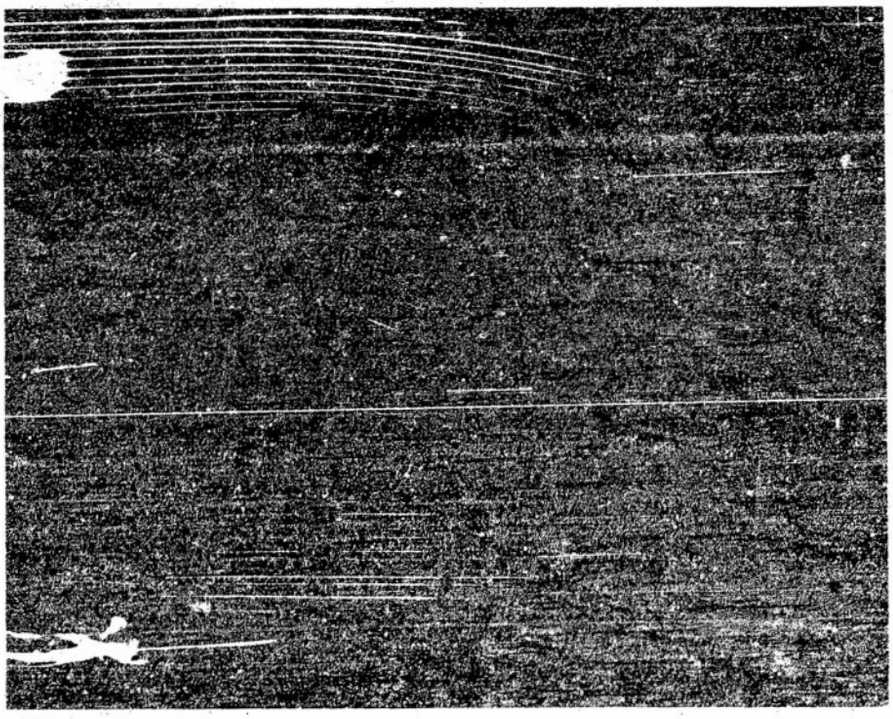

FIG. 9

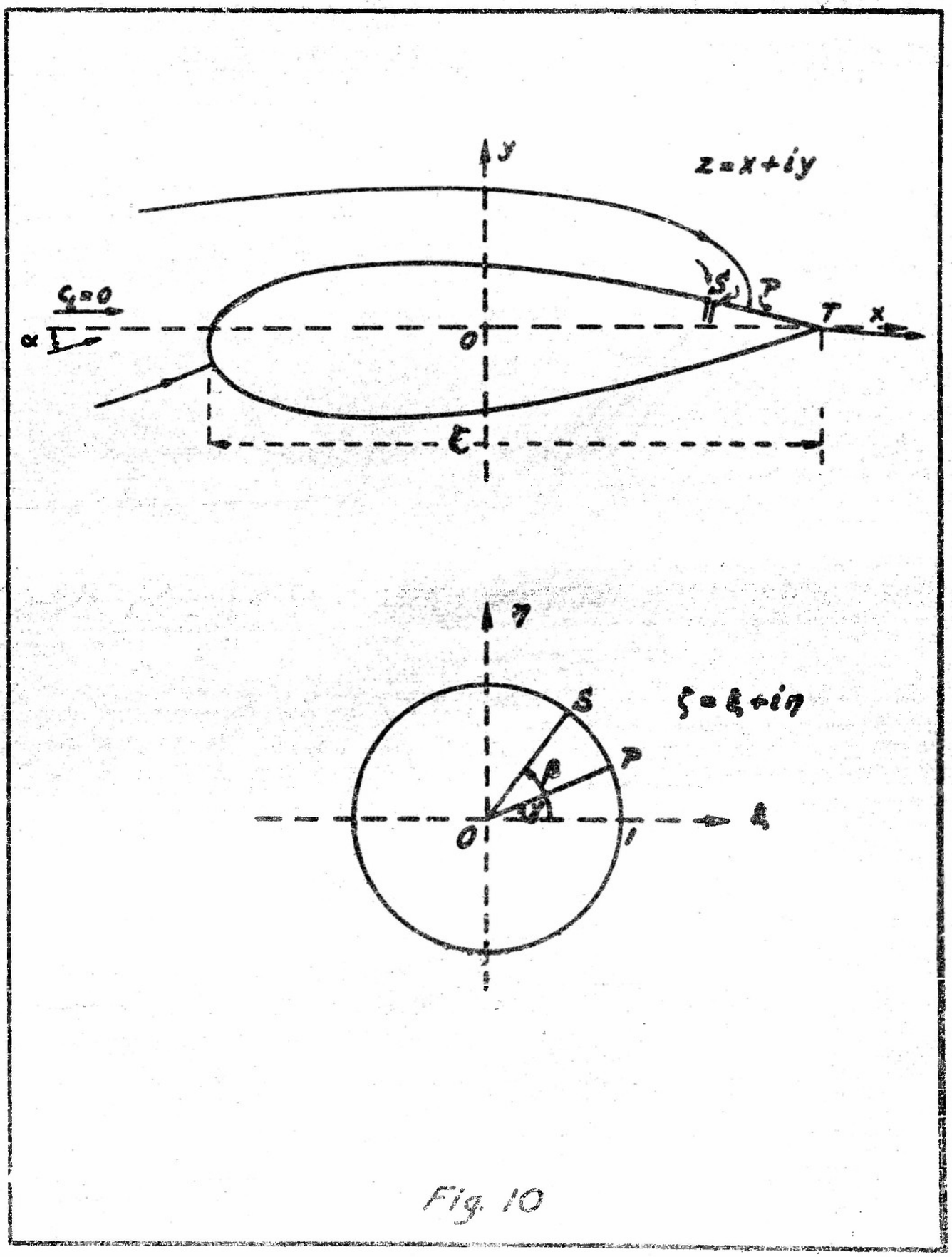

Fig. 10

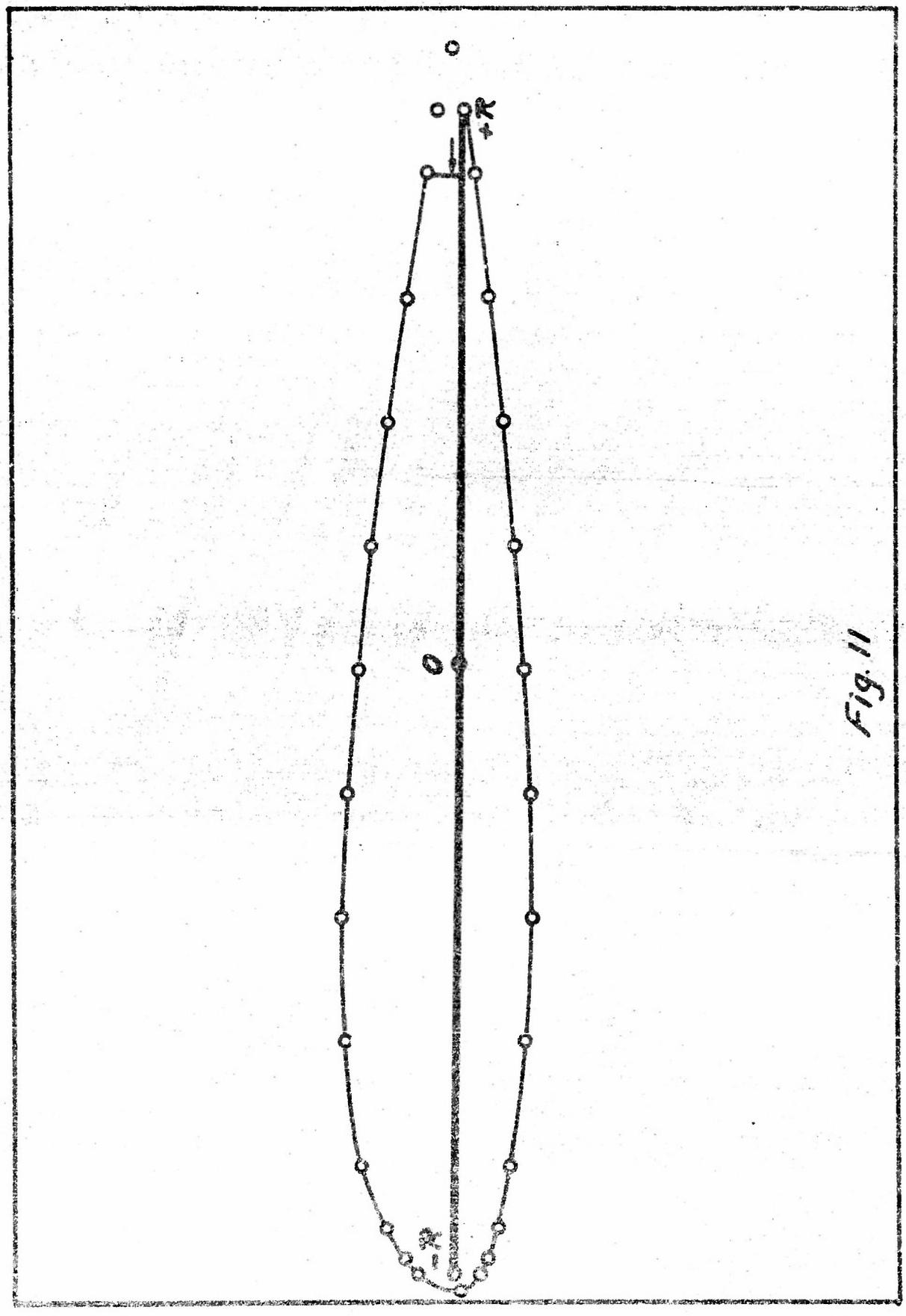

Fig. 11

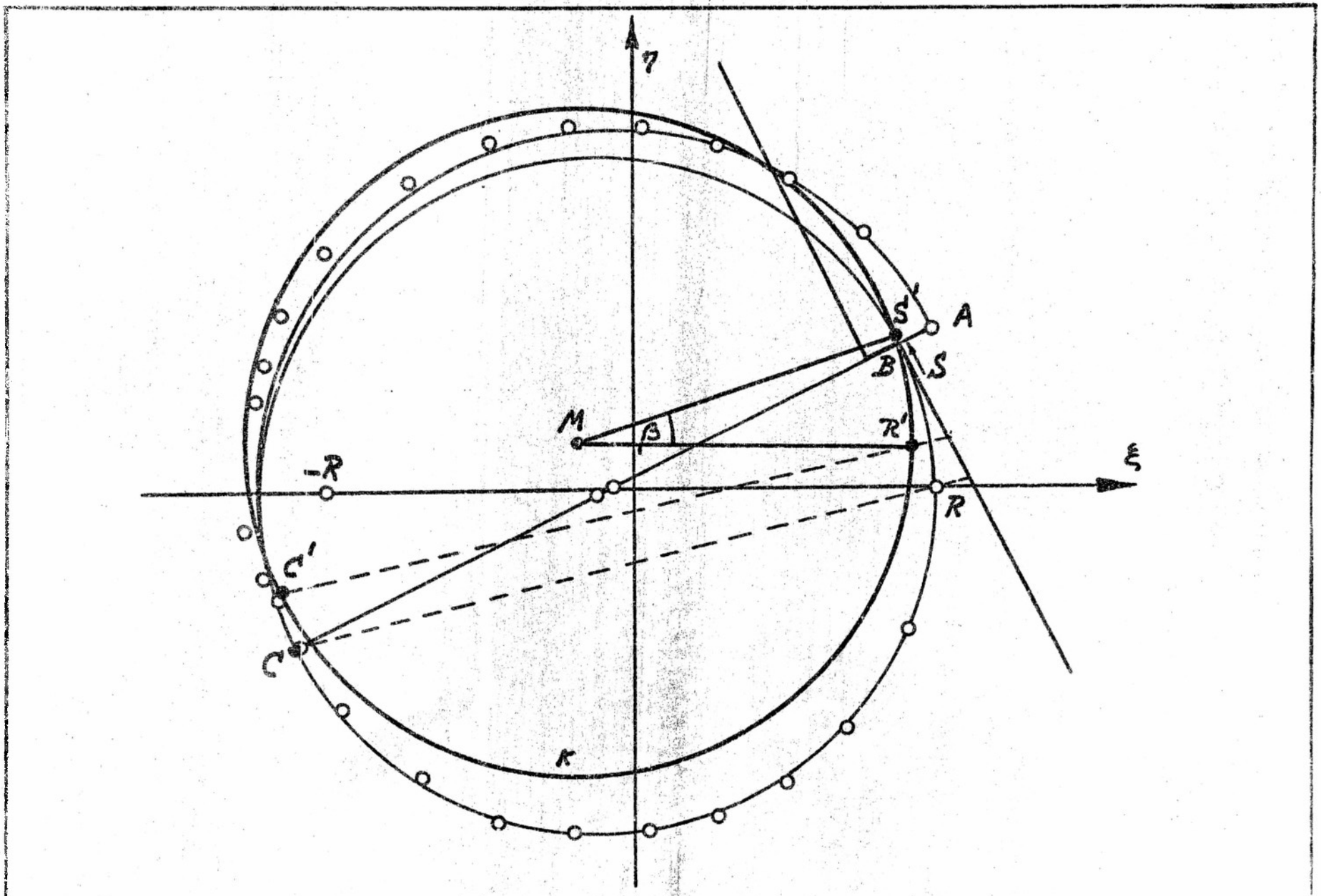

Fig. 12

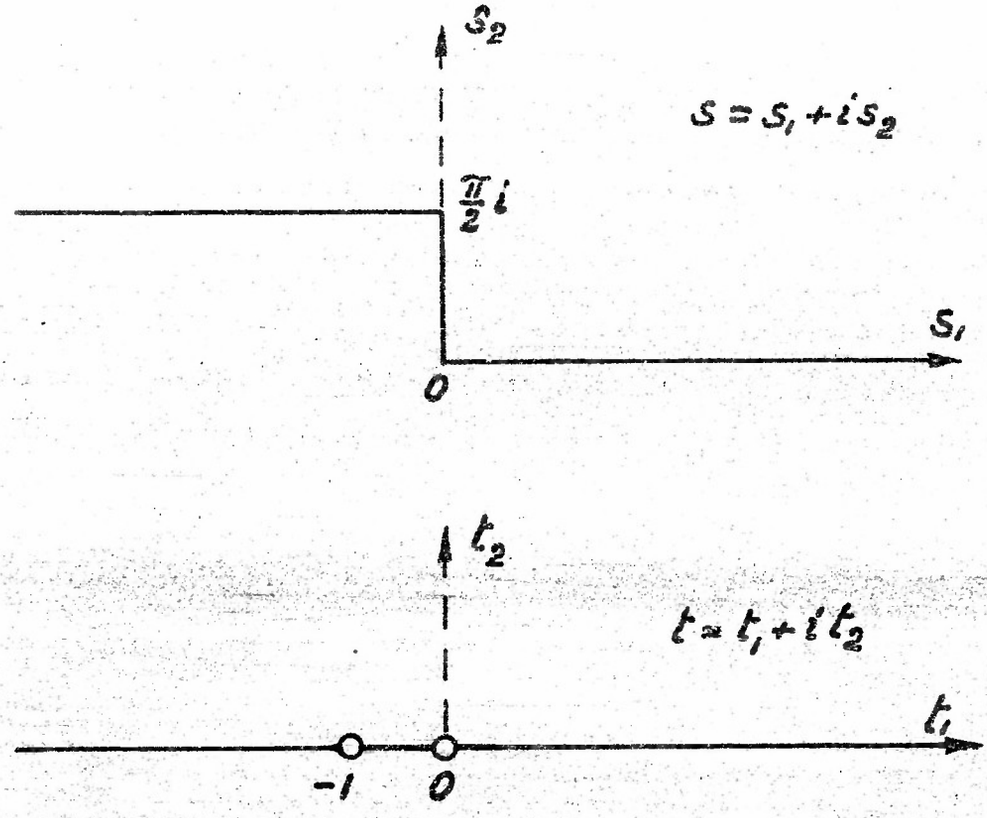

Fig. 13

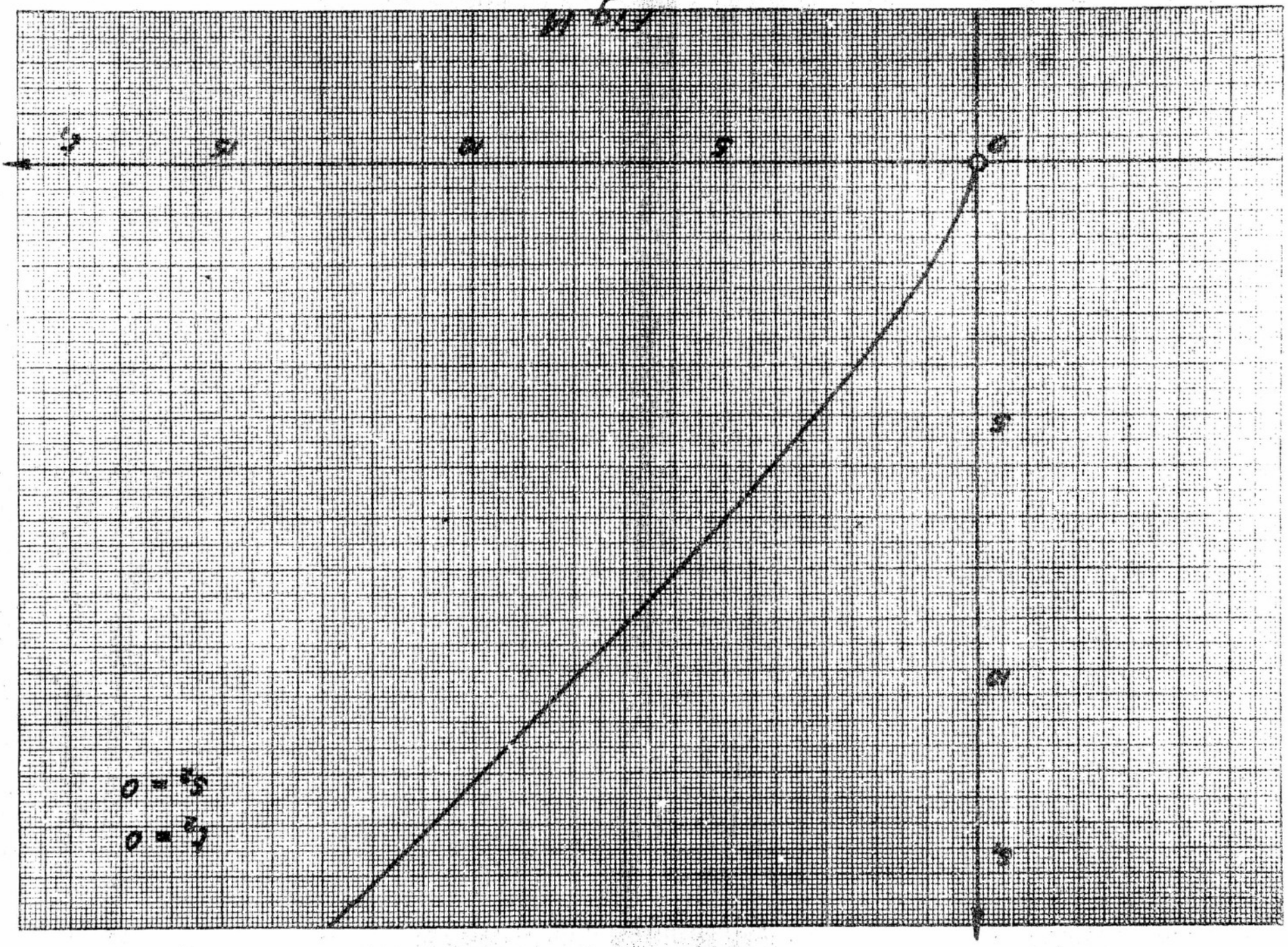
Fig 4
$\sigma = \epsilon_S$
$\sigma = \epsilon_y$

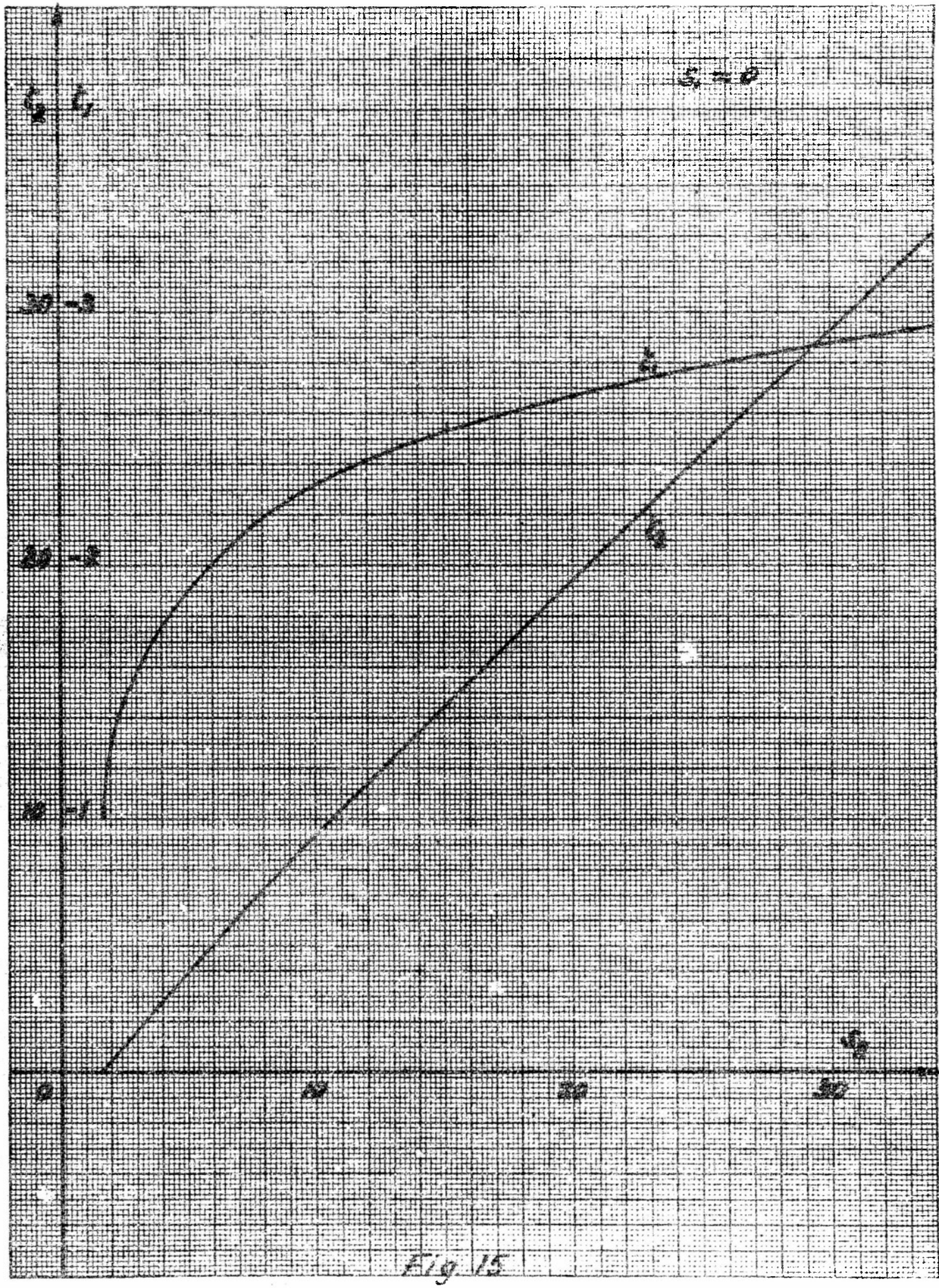

Fig 15

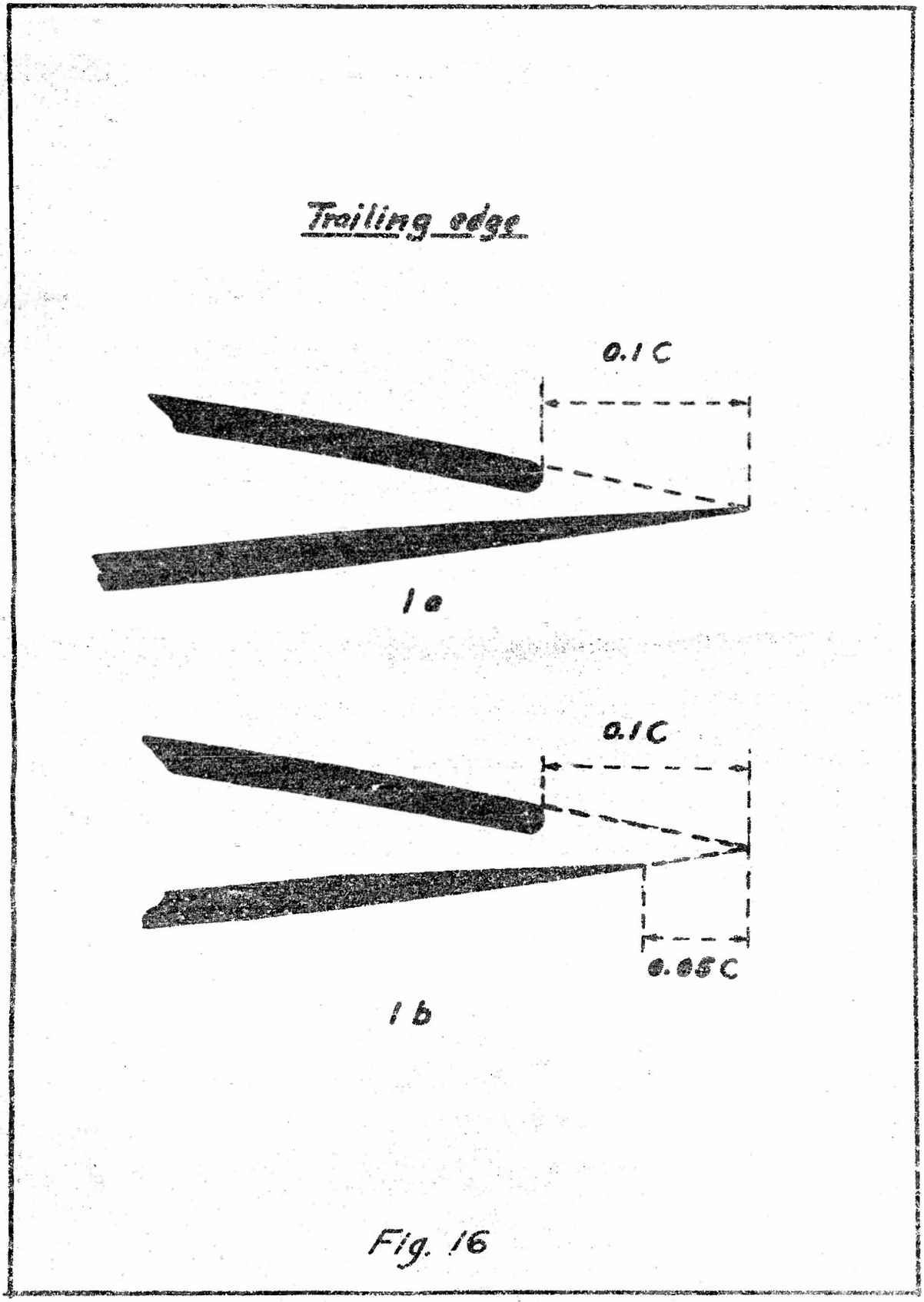

Fig. 16

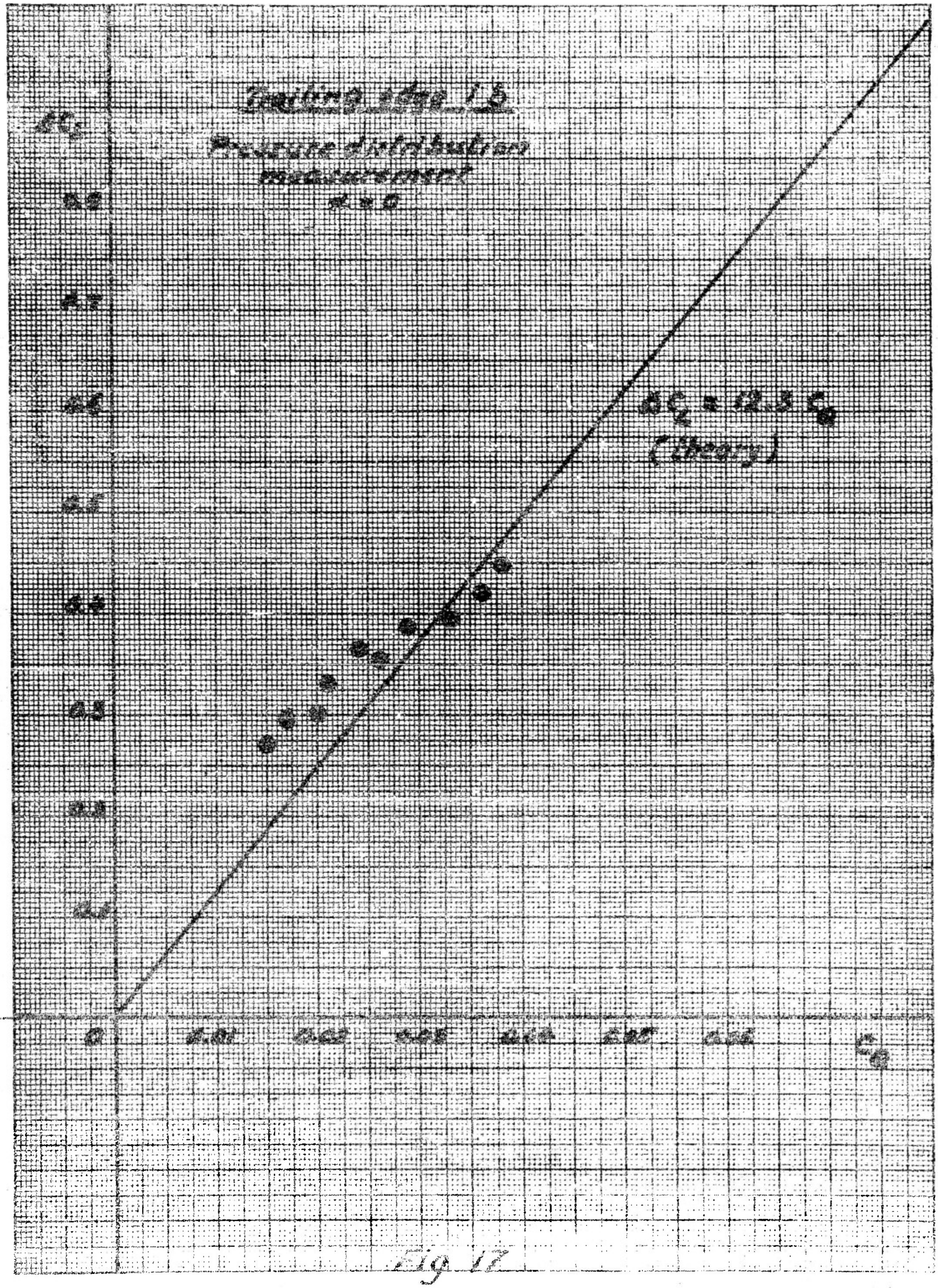

Fig 12

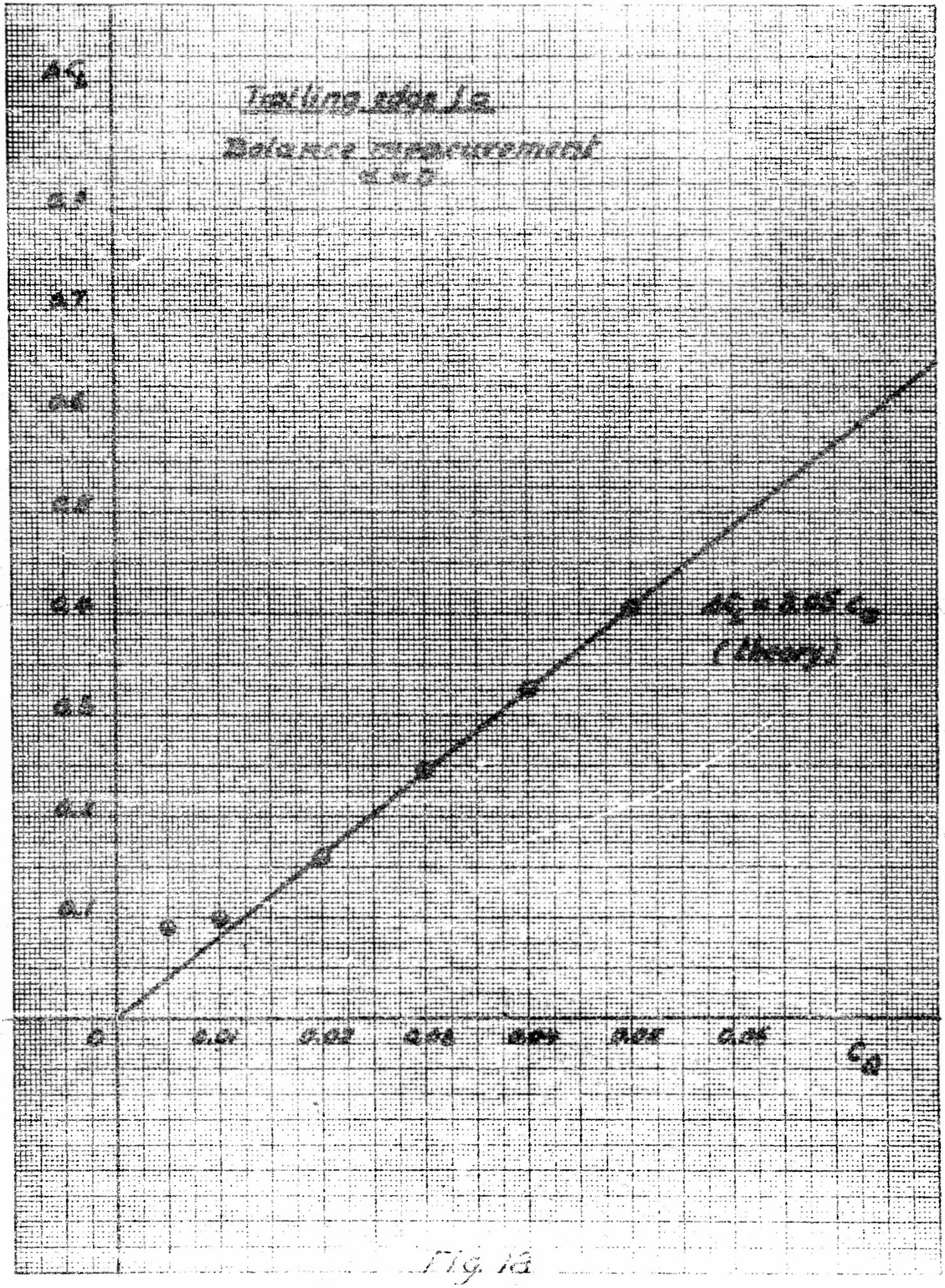
Testing with Le
Balance measurement
$\alpha = 0$
C_L
C_D
$C_L = 2\pi \sin^2 \alpha_0$
(theory)

Fig. 18

COMPARISON OF THEORETICAL AND EXPERIMENTAL PRESSURE DISTRIBUTIONS

$\alpha = 0$, $c_{l_0} = .0285$, $c_l = 0.387$

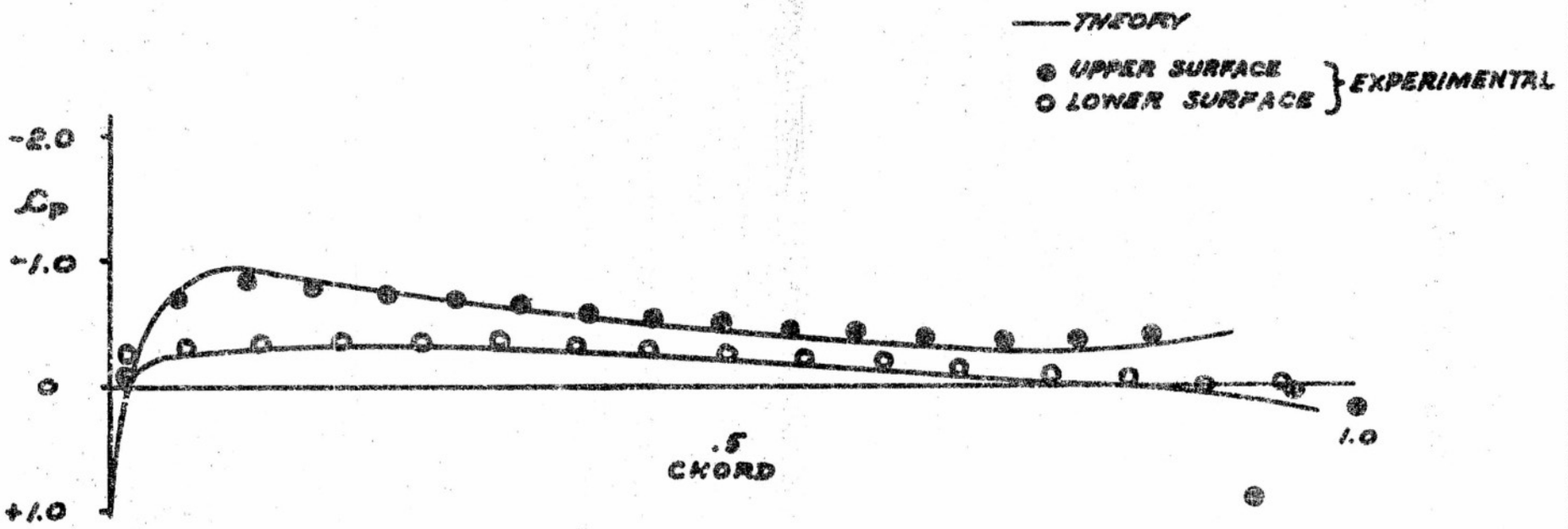

Fig. - 19

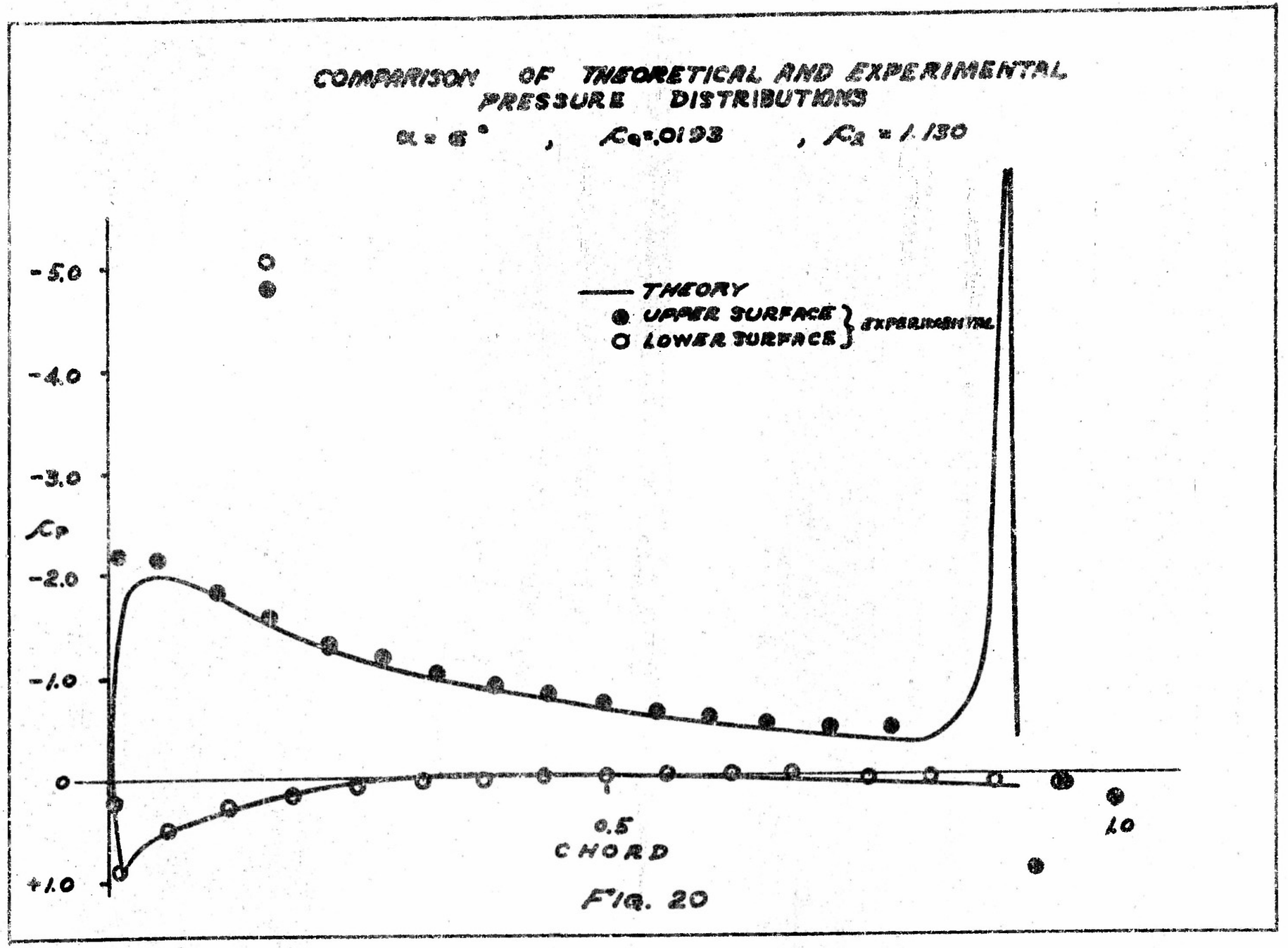
COMPARISON OF THEORETICAL AND EXPERIMENTAL PRESSURE DISTRIBUTIONS
α = 6°, c_{l_0} = .0193, c_{l_2} = 1.130
THEORY
UPPER SURFACE
LOWER SURFACE
EXPERIMENTAL
-5.0
-4.0
-3.0
c_p
-2.0
-1.0
0
+1.0
0.5
CHORD
1.0

FIG. 20

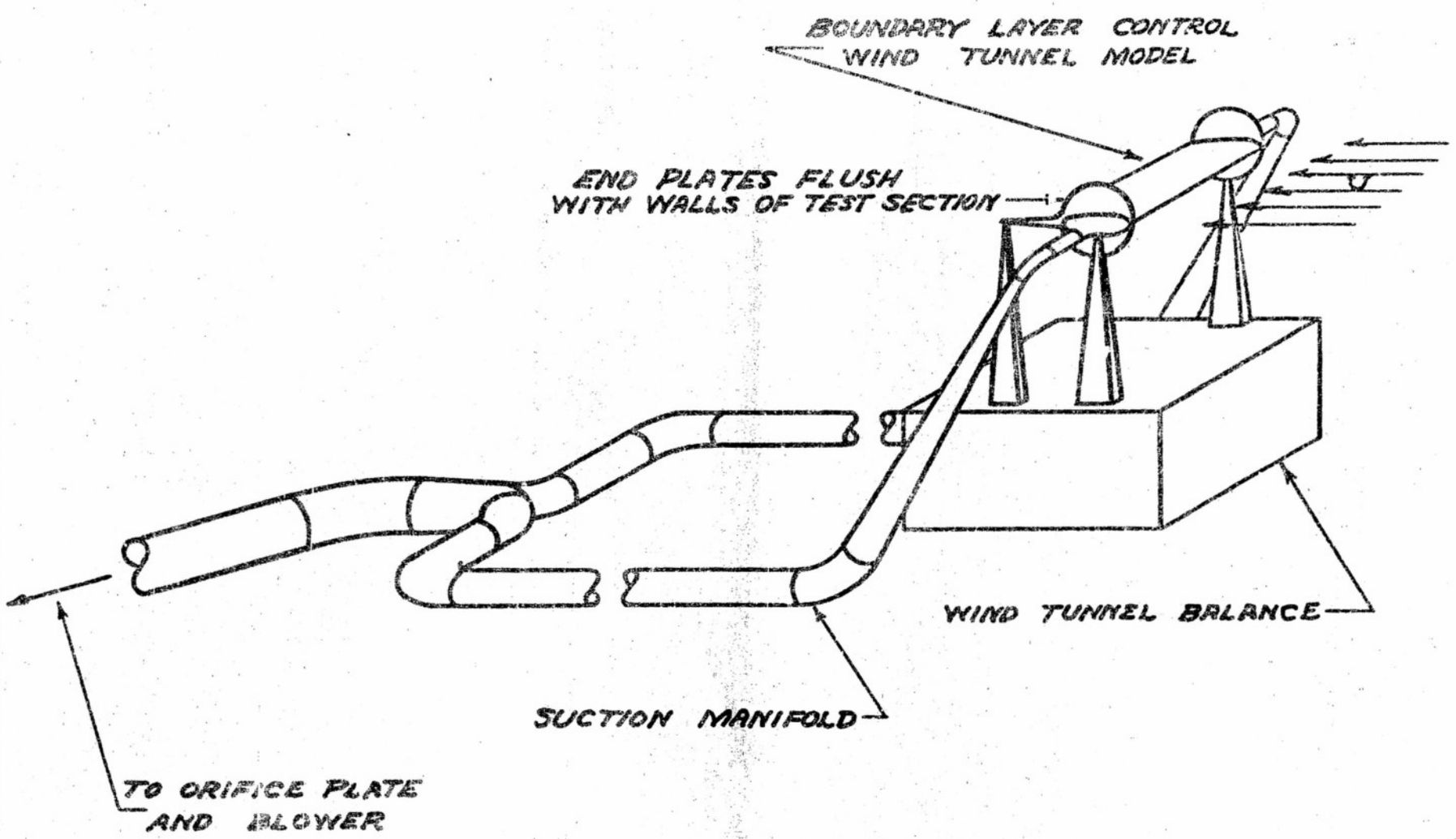

FIG. ~ 21

SCHEMATIC DIAGRAM OF
MODEL, BALANCE AND BLOWER INDUCTION SYSTEM

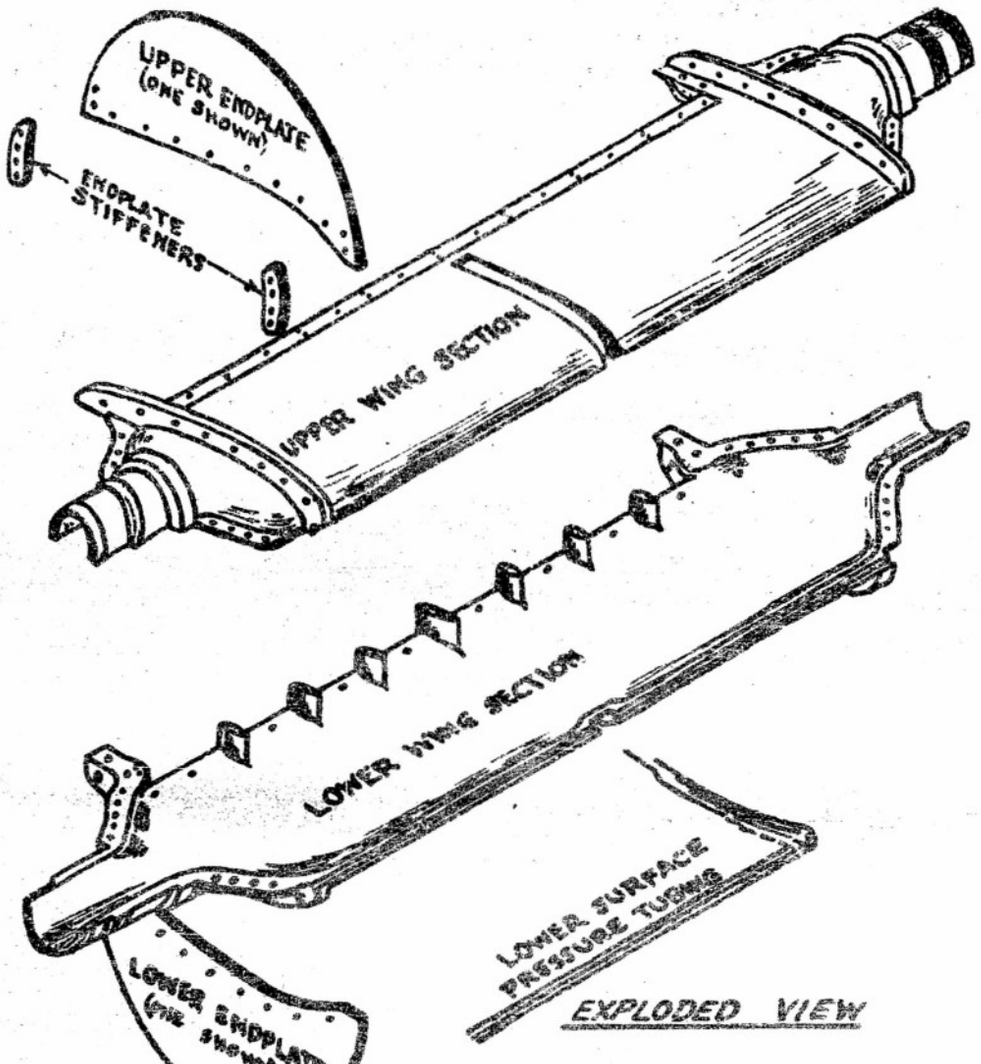

EXPLODED VIEW

Boundary Layer Control Wind Tunnel Model

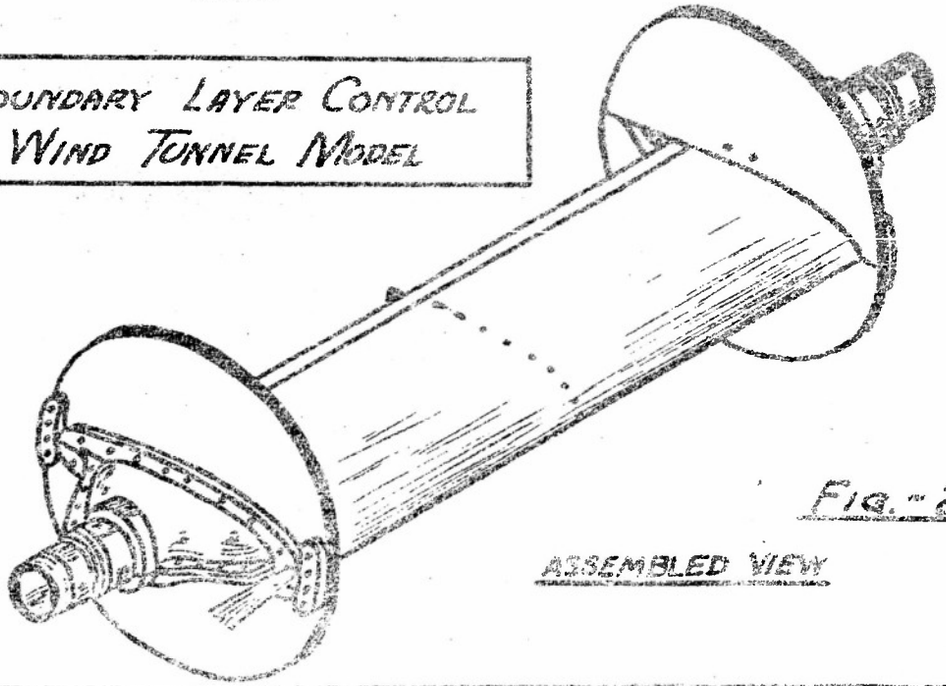

ASSEMBLED VIEW

Fig. - 22

NACA 23015 AIRFOIL AS MODIFIED FOR TRAILING EDGE SUCTION TESTS

FIG.-23A

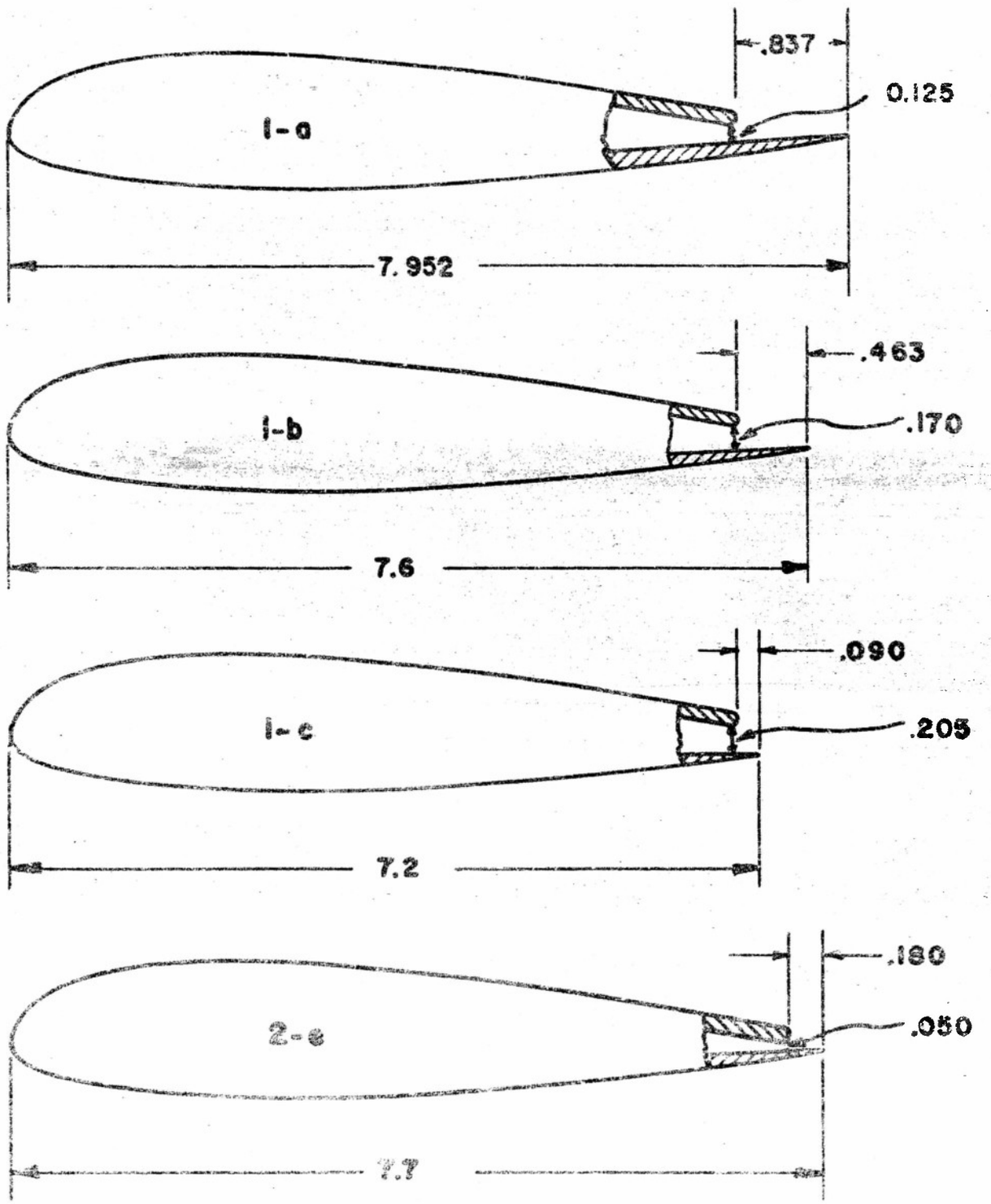

NACA 23015 AIRFOIL AS MODIFIED FOR TRAILING EDGE SUCTION TESTS

FIG. 238

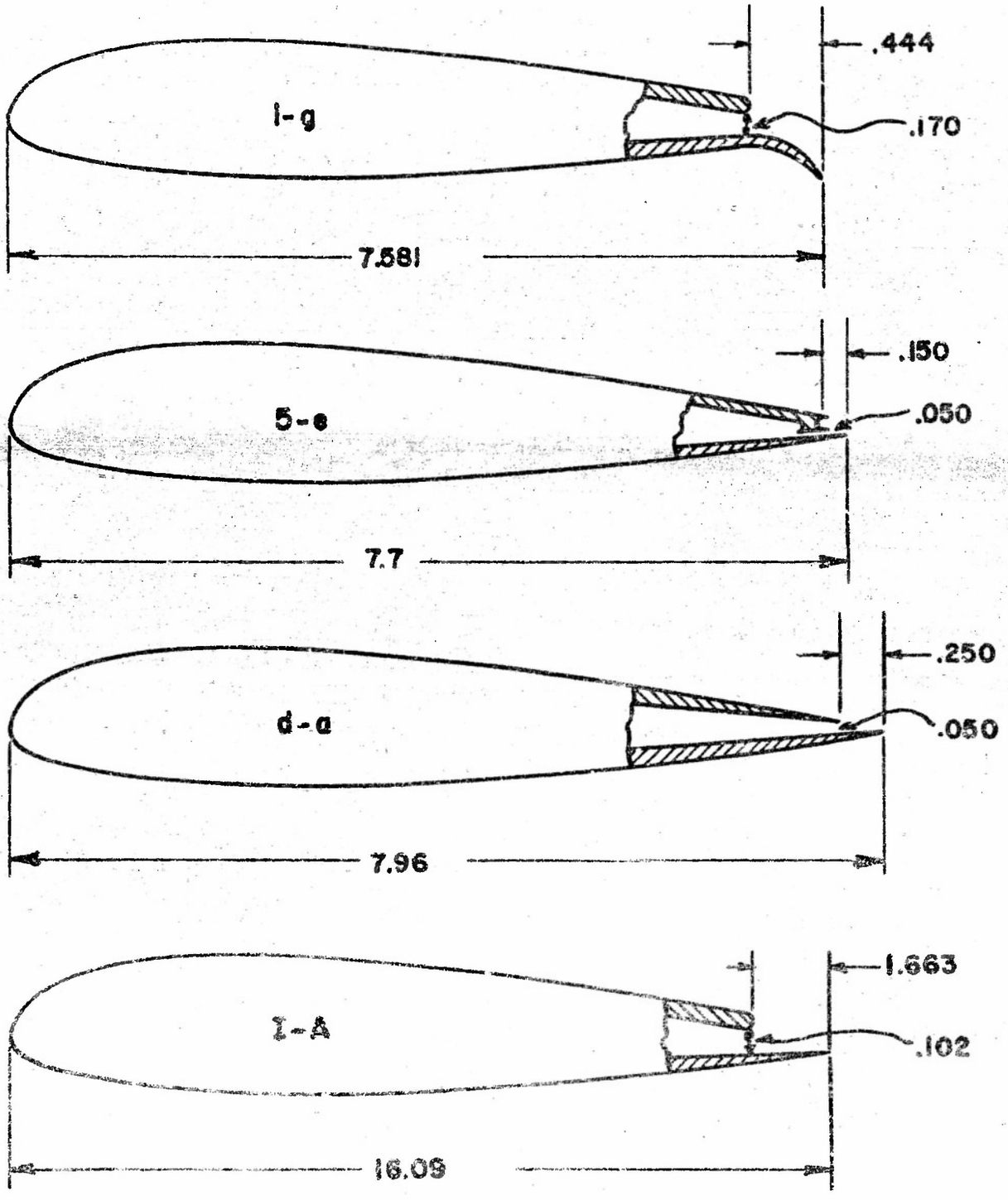

NACA 23015 AIRFOIL AS MODIFIED FOR TRAILING EDGE SUCTION TESTS

FIG. 23C

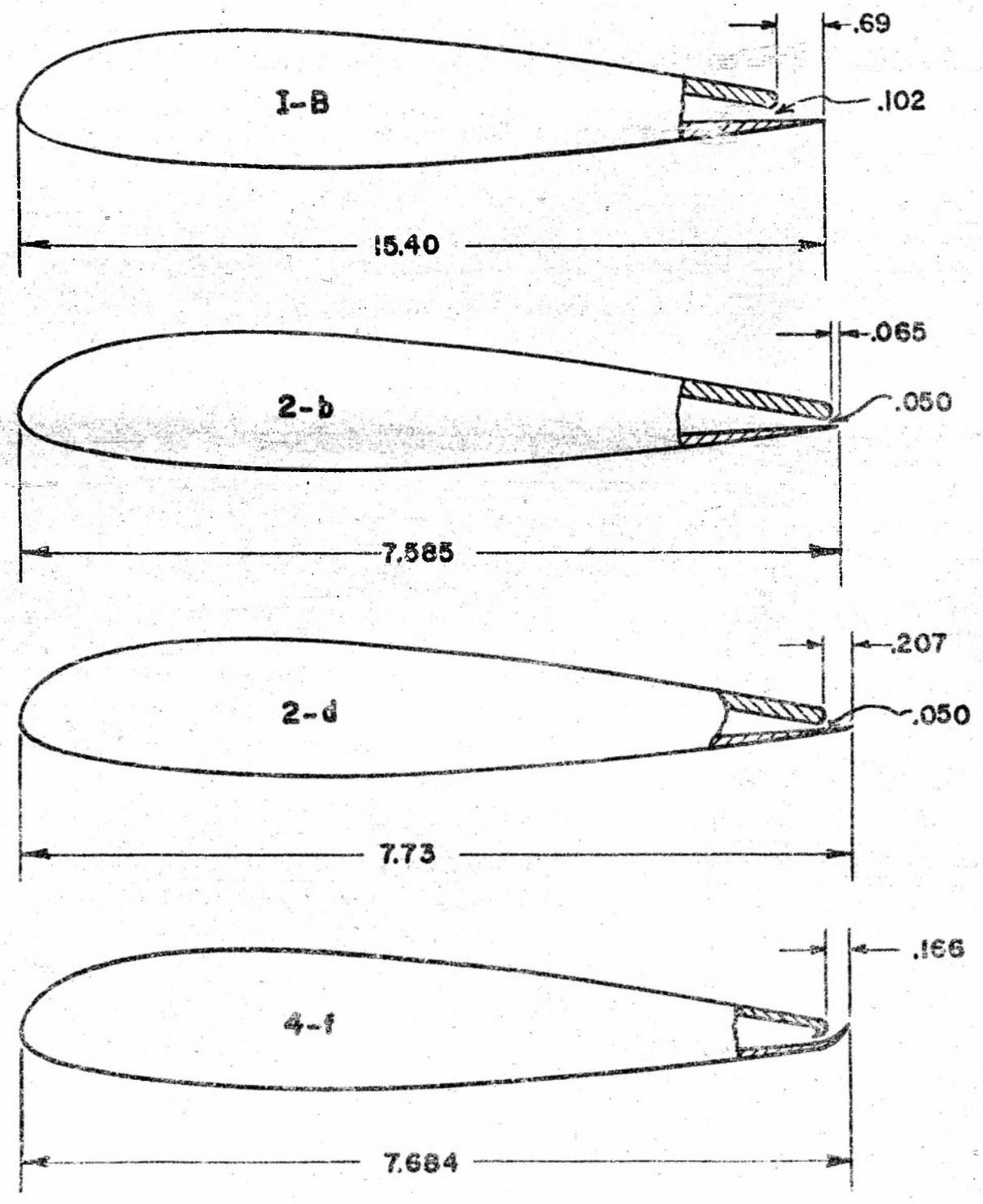

SUMMARY OF TRAILING EDGES TESTED RELATED TO $C_{l\,MAX.}$ AND C_q

NACA 23015 AIRFOIL

FIG. ~ 24

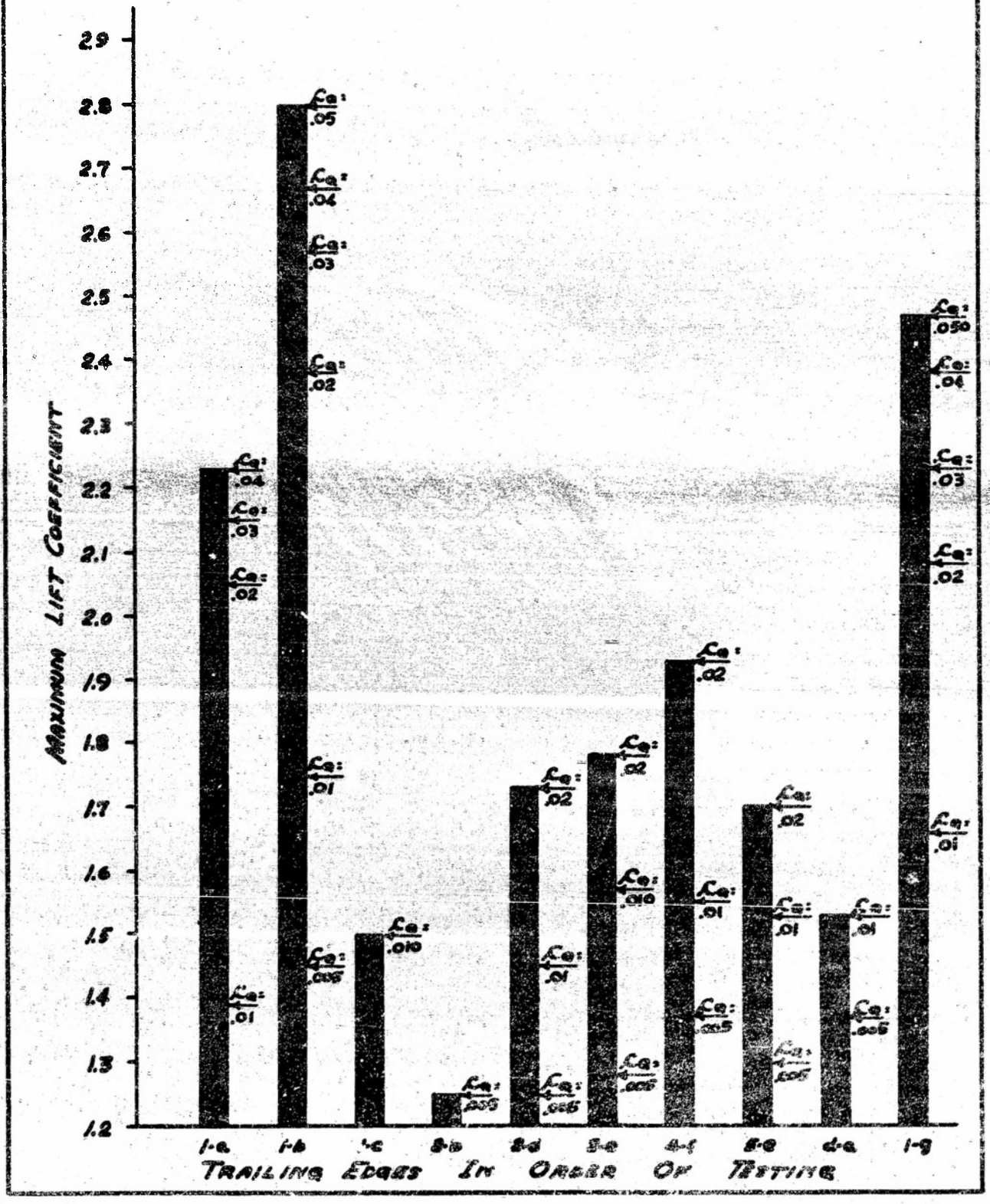

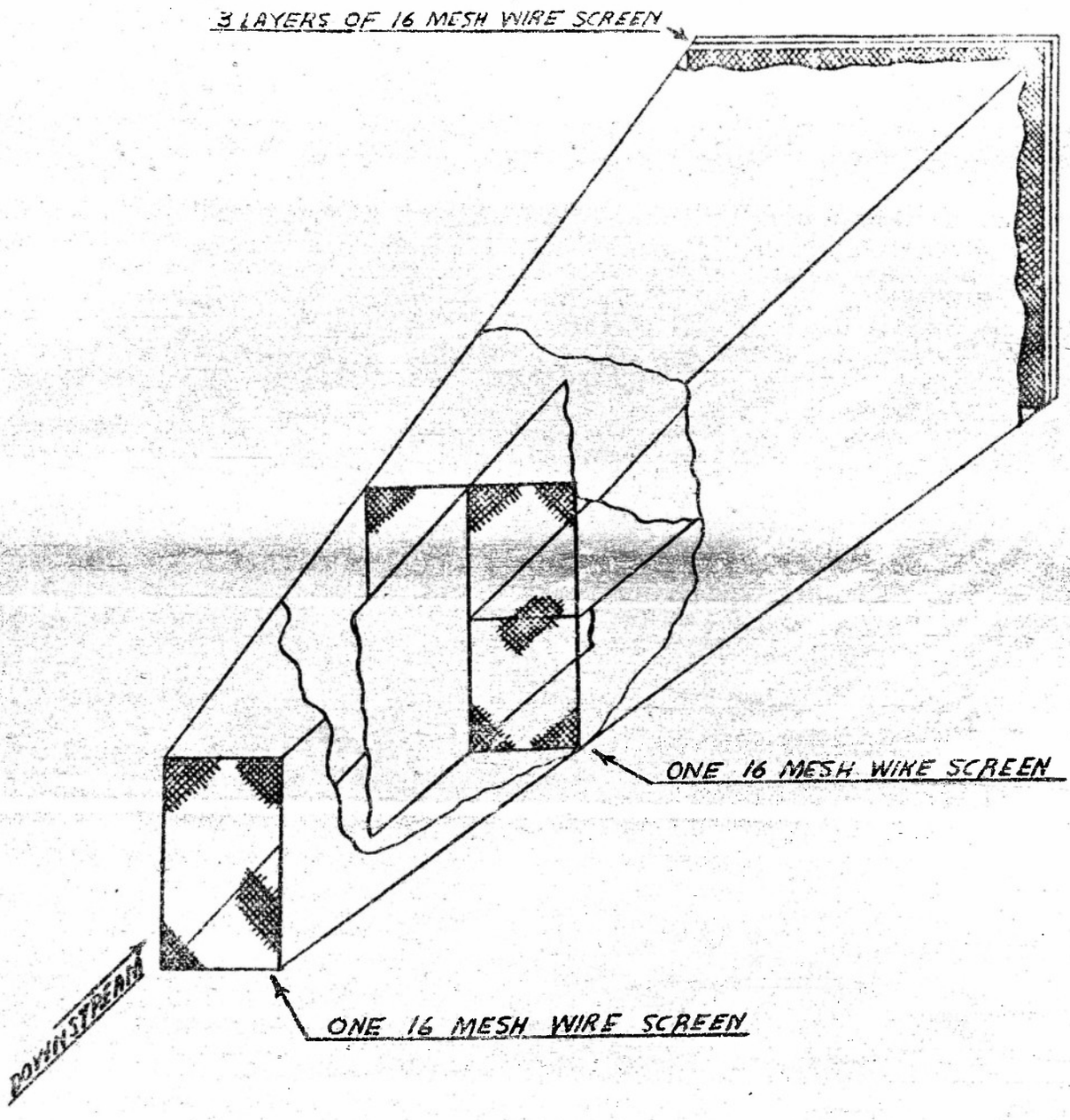

FIG.-25

SCHEMATIC ARRANGEMENT OF SCREENS IN DIFFUSER

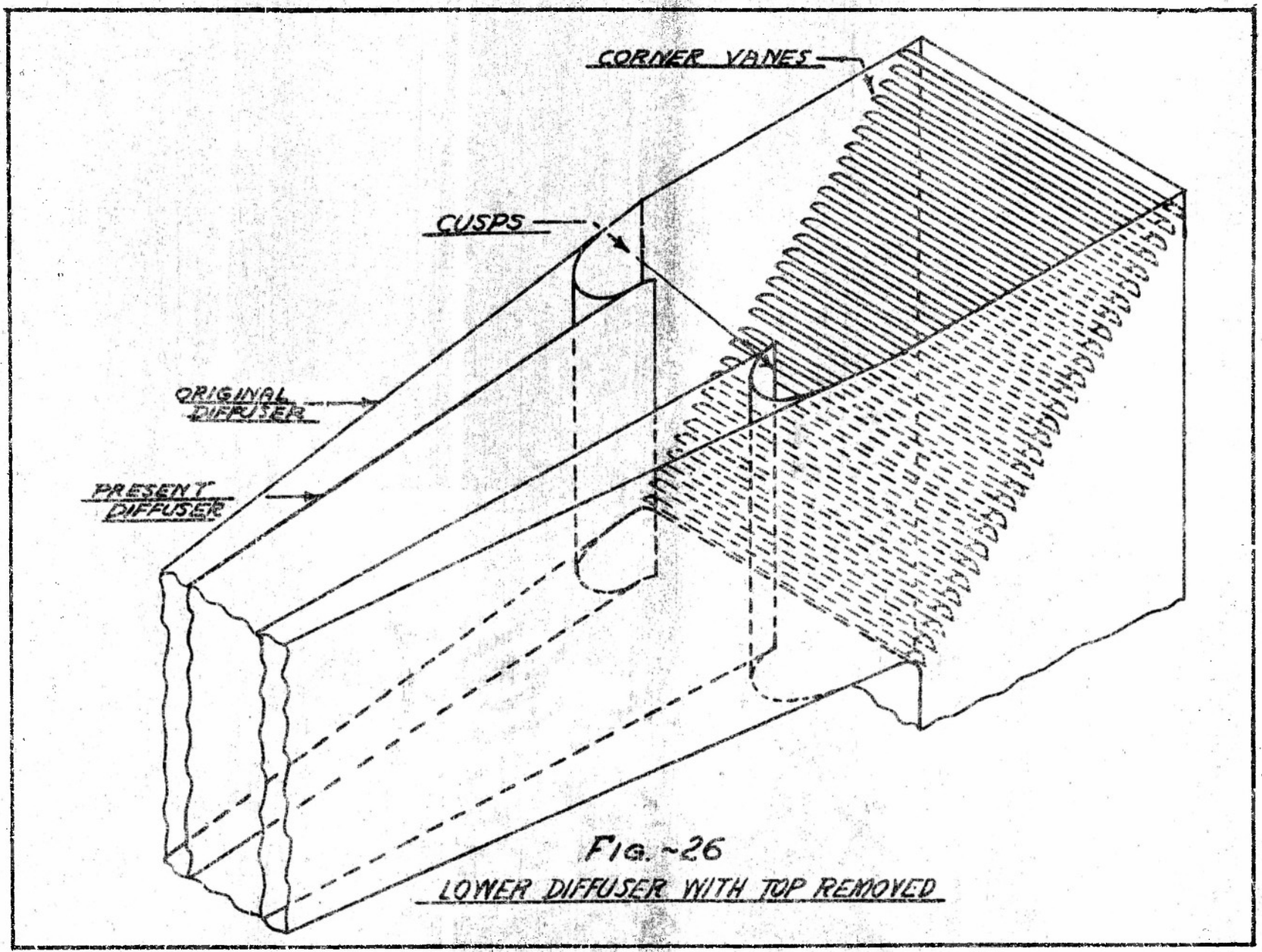

FIG.-26
LOWER DIFFUSER WITH TOP REMOVED

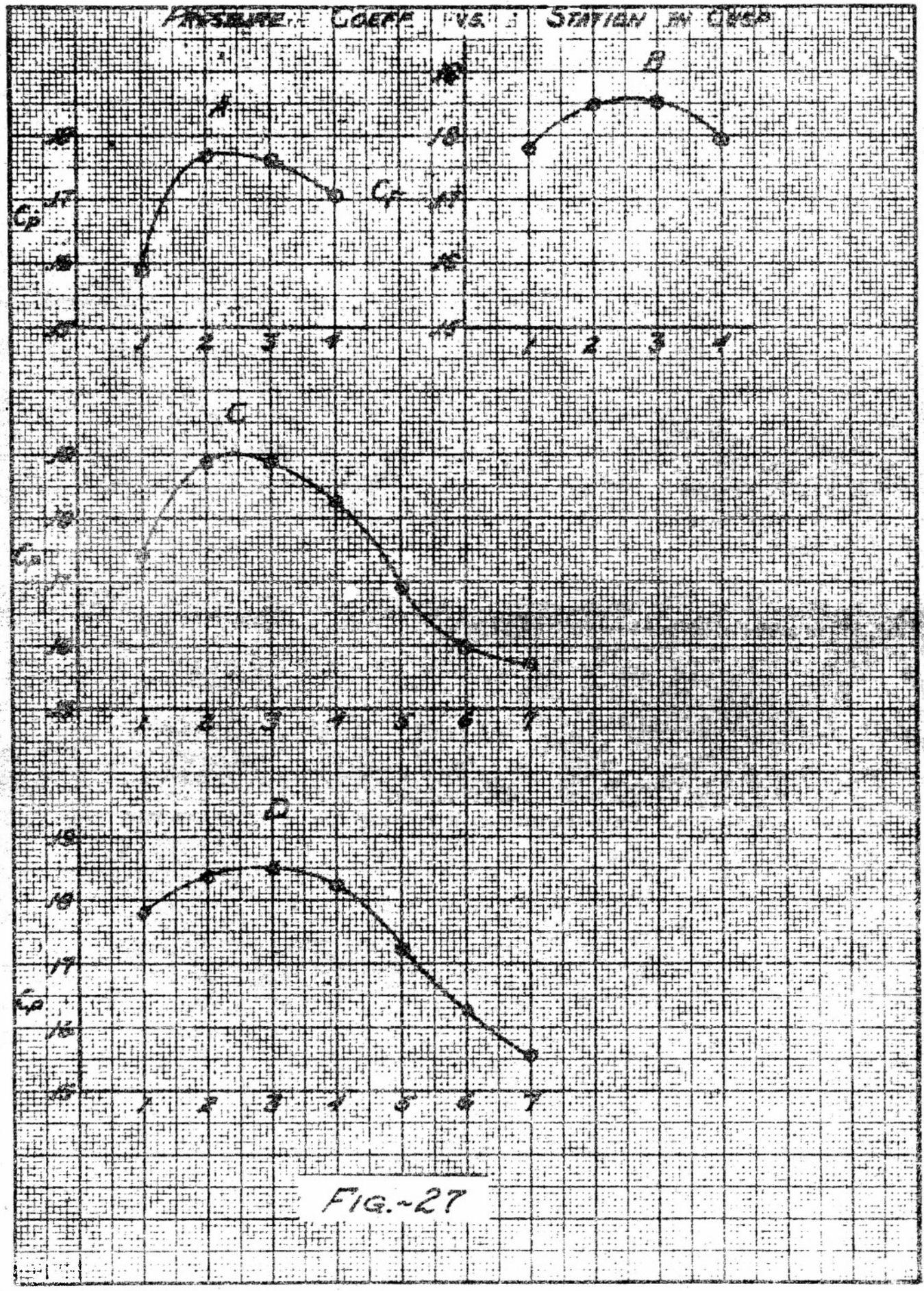

FIG.-27

LOCATION OF PRESSURE TAPS IN CUSP

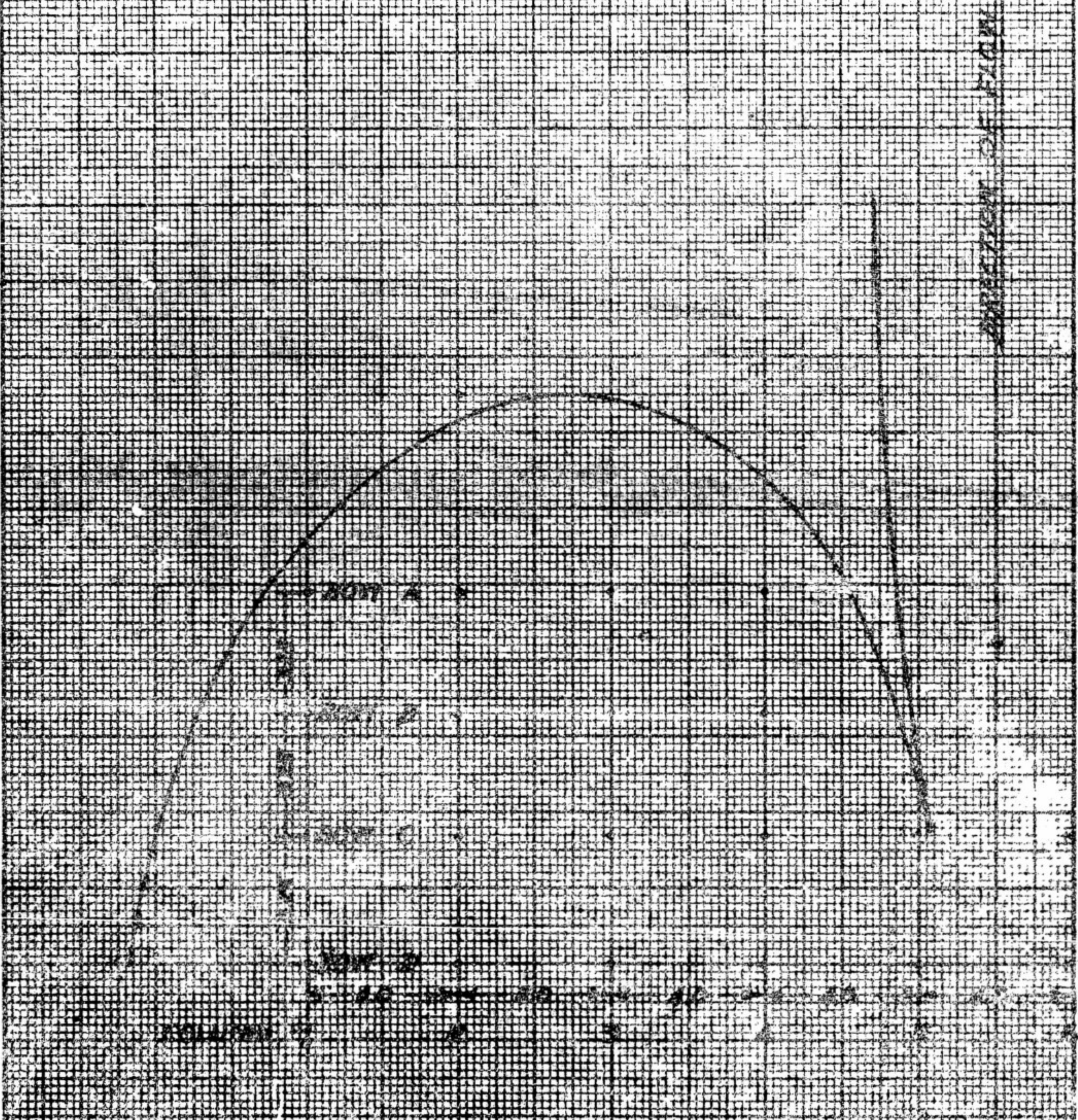

FIG.-28

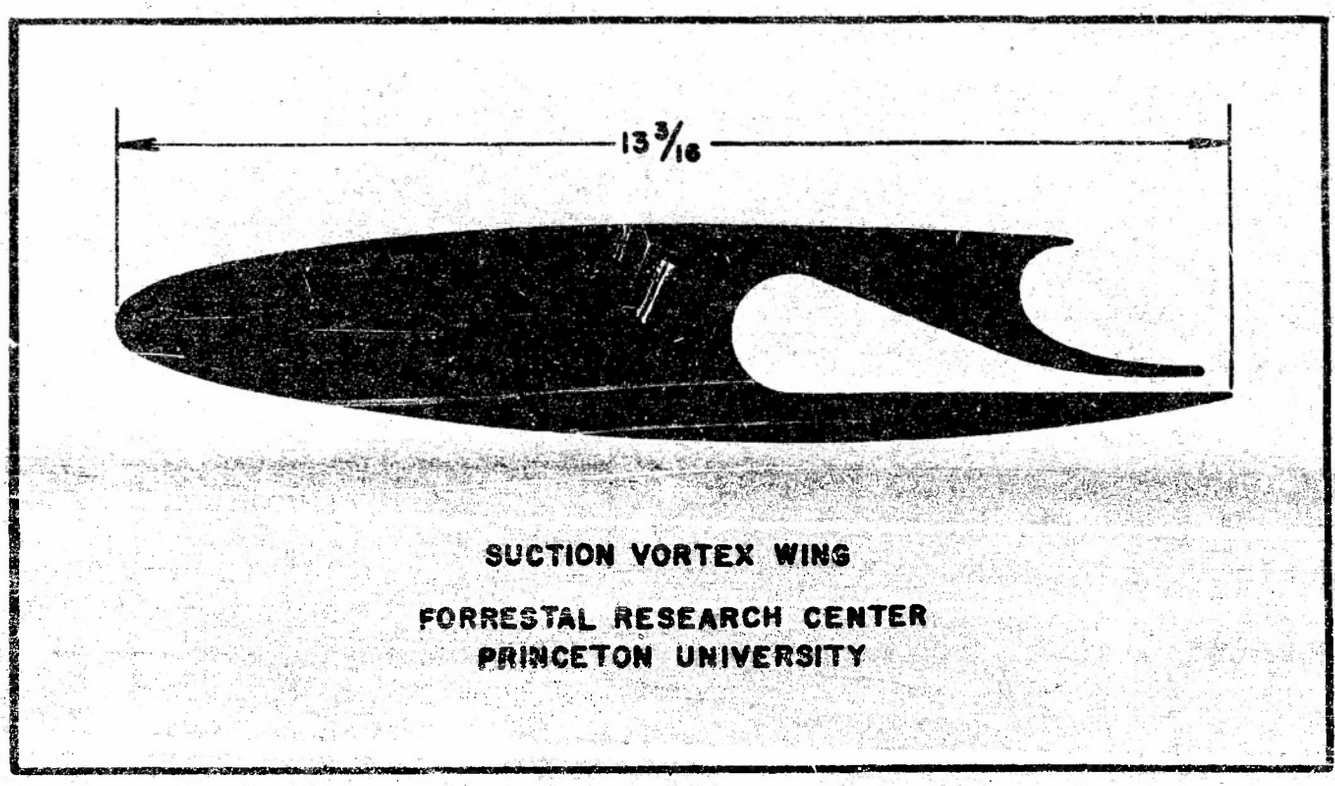
13 3/16
SUCTION VORTEX WING
FORRESTAL RESEARCH CENTER
PRINCETON UNIVERSITY

FIG. 29

PRESSURE DISTRIBUTIONS FOR SUCTION VORTEX WING

▲ - LOWER SURFACE
● - UPPER SURFACE

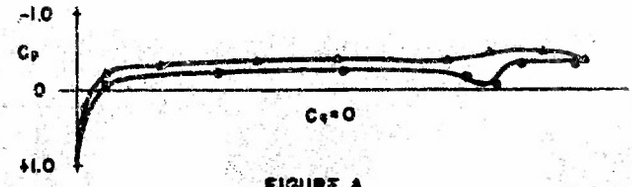

FIGURE A

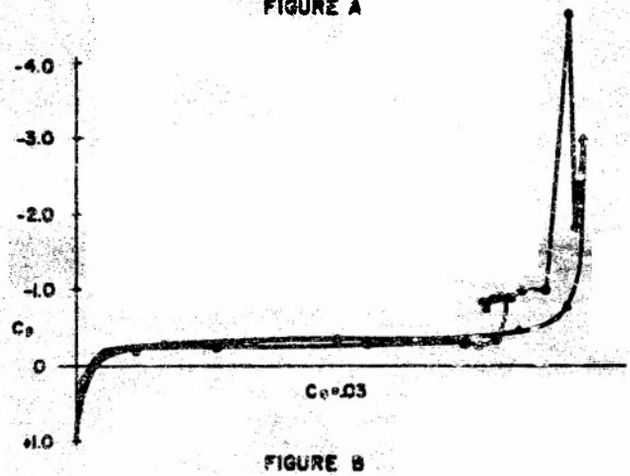

FIGURE B

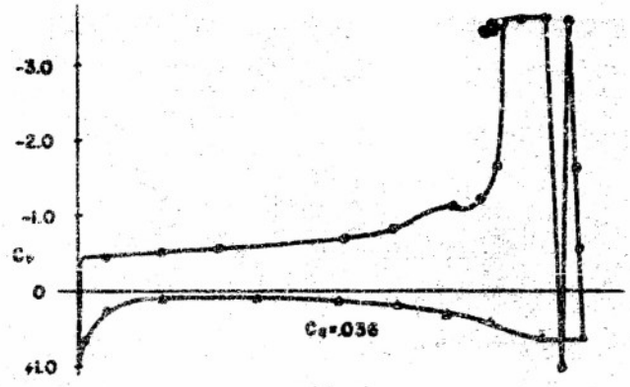

FIGURE C

FORRESTAL RESEARCH CENTER PRINCETON UNIVERSITY

FIG. 30